Spring 2008

Derivation of the respiratory rate signal from a single lead ECG

Murtaza M. Lakdawala
New Jersey Institute of Technology

ABSTRACT

DERIVATION OF THE RESPIRATORY RATE SIGNAL FROM A SINGLE LEAD ECG

by

Murtaza M. Lakdawala

It has been long established that respiration has an influence on heart rate, and this effect is called respiratory sinus arrhythmia. As a result, two inferences can be postulated: first respiration information can be derived from cardiac activity, and second this effect offers the potential of removing the respiration effect that suppresses cardiac information which is of clinical significance. As a result of research performed at NJIT, there is a significant amount of data on exercise and heart rate recovery, but not the associated respiration signal. The motivation of this research was to compare and implement an optimal ECG derived respiration program, develop an adaptive peak detector algorithm to process the complex respiration signal and produce a usable respiration rate waveform. Three methods for deriving respiration from a single lead ECG were identified and implemented in LabVIEW. The three methods were R wave amplitude modulation (RWA), R wave duration (RWD), and the multiplication of RWA and RWD signals. Data analysis was carried out by comparing actual paced breathed respiration signal with lead I ECG derived respiration of ten normal subjects. The data analysis suggests that RWA is the best method with a correlation of 0.95. Then an algorithm to derive a continuous respiration rate signal from actual respiration signal with a high level of accuracy was developed. As a result of this research a program has been developed which provides respiratory information of clinical significance from ordinary single lead ECG for situations in which ECG but respiration is not routinely monitored.

DERIVATION OF THE RESPIRATORY RATE SIGNAL FROM A SINGLE LEAD ECG

by

Murtaza M. Lakdawala

A Thesis
Submitted to the Faculty of
New Jersey Institute of Technology
in Partial Fulfillment of the Requirements for the Degree of
Master of Science in Biomedical Engineering

Department of Biomedical Engineering

May 2008

APPROVAL PAGE

DERIVATION OF THE RESPIRATORY RATE SIGNAL FROM A SINGLE LEAD ECG

Murtaza M. Lakdawala

5/5/08

Dr. Ronald H. Rockland, Thesis Advisor — Date
Professor, Engineering Technology/Biomedical Engineering, NJIT

5/5/08

Dr. Joel Schesser, Committee Member — Date
University Lecturer, Biomedical Engineering, NJIT

5/01/08

Dr Mesut Sahin, Committee Member — Date
Assistant Professor, Biomedical Engineering, NJIT

BIOGRAPHICAL SKETCH

Author: Murtaza Mahammadali Lakdawala

Degree: Master of Science

Date: May 2008

Undergraduate and Graduate Education:

- Master of Science in Biomedical Engineering,
  New Jersey Institute of Technology, Newark, NJ, USA, 2008

- Bachelor of Engineering in Biomedical & Instrumentation Engineering,
  C. U. Shah College of Engineering & Technology, Wadhwan City, Gujarat, India, 2006

Major: Biomedical Engineering

To my mummy & papa, the fountains of my inspiration

ACKNOWLEDGMENT

I would like to thank Dr. Ronald Rockland for being my mentor and thesis advisor. His vision and knowledge helped me accomplish the challenging research. I express my sincere thanks to Dr. Joel Schesser for giving me valuable tips that helped me throughout my research and for being in my thesis committee. I thank Dr. Mesut Sahin for participating in my thesis committee.

I am grateful to Dr. Tara Alvarez and Dr. Sina Zaim for providing me with the physiological data for the research.

I take this opportunity to thank all my friends here and in India, who have been there for me in good times and bad, who instilled in me the confidence and courage to move forward. I thank a special someone who was never around, but was always by my side. I lovingly thank my parents and my brother Kausar for their support. Finally, I offer my humble thanks to The Almighty, Allah.

TABLE OF CONTENTS

TABLE OF CONTENTS
(Continued)

Chapter **Page**

LIST OF TABLES

LIST OF FIGURES

LIST OF FIGURES
(Continued)

LIST OF FIGURES
(Continued)

CHAPTER 1

OBJECTIVE

Knowledge of respiratory patterns would be clinically useful in many situations in which the ECG, but not respiration, is routinely monitored [1]. Respiration is the most important modulator of heart rate, and the source of the short term heart rate variability. Analysis of ECG with respect to respiration can give important insight into the autonomic control of heart rate. Several methods exist to measure respiration indirectly through thoracic movements or electrical impedance measurement [2]. Direct measurement of air flow through the mouth and nose is considered to be the gold standard which is usually done by temperature measurement of inhaled and expelled air.

The objective behind the implementation of ECG derived respiration is to be able to measure respiration from an available ECG source without the use of additional hardware, or produce a respiration signal from recordings that only contain single lead ECGs. The respiration rate signal, derived from the respiration signal, is an important part of heart rate variability (HRV) analysis. Being able to produce that signal from single lead ECGs is critical for accurate HRV analysis.

The EDR method is based on small changes in ECG morphology during the respiratory cycle caused by movement of the heart position relative to the electrodes and the change of lung volume [3]. A number of algorithms for estimating respiration from single and multi-lead ECGs have been reported [4], [5], [6]. Methods for deriving respiration from a single lead ECG are identified and implemented in this thesis using LabVIEW. The first method, called R-wave amplitude modulation (RWA), is based on

the fact that respiration causes detectable change in amplitude of R waves. The second method, called the R-wave duration (RWD), is based on the change in area under the R-wave due to respiratory efforts. A comparison of these methods will be performed on a set of data that contains both respiration and heart rate by analyzing the difference between the respiration rate signal from the actual respiration signal and the derived respiration signal.

CHAPTER 2

BACKGROUND RESEARCH

2.1 Electrophysiology of Heart

2.1.1 Conductive System of the Heart

The recording of the electrical activity of the heart is known as an electrocardiogram (ECG). An ECG is a quasi-periodical, rhythmically repeating signal synchronized by the function of the heart, which acts as a generator of bioelectric events. This signal can be described by means of an electric dipole. The dipole generates a field vector which changes periodically in time and space and its effects can be measured on the surface of the body. The ECG waveforms have been standardized in terms of amplitude and phase relationships and any deviation from this reflects the presence of an abnormality [7].

The heart (see Figure 2.1) has its own system of generating and conducting action potentials through a complex change of ionic concentration across the cell membrane. The Sino-atrial node (SA node) is the pacemaker of the heart and it is a group of cells located in the top right atrium near the entry of the vena cava that excite the muscles of the heart [8]. The SA node generates impulses at a normal rate of about 72 beats per minute. As the body acts as a resistive medium, these impulses propagate through the conductive cells to other parts of the heart. The excitation wave travels through the right and left atria at a velocity of about 1m/s and about 0.1s is required to complete the atrial excitation. This action potential contracts the atrial muscle and travels to the Atrio-ventricular node (AV node) located in the lower part of the wall between the two atria in about 0.04s. A fibrous barrier of non-excitable cells called the Purkinje fibers in the AV

node delays the spread of potential for about 0.11s [9]. The potential is then carried to the ventricles by a special conduction system called the bundle of His. Thus, the AV node and bundle of His functionally connects the atria and ventricles. The AV node delay ensures that the atria complete their contraction before ventricular contraction takes place. Also, the Purkinje fibers split into two branches to simultaneously excite the two ventricles. Conduction velocity of the action potentials in Purkinje fibers is about 1.5 to 2.5 m/s. Since the direction of the impulse propagating in the bundle of His is from the apex of the heart, ventricular contraction starts from the apex and continues upwards through the ventricular walls. This causes a squeezing action of the ventricles which pumps the blood out of the ventricles into the aorta [10].

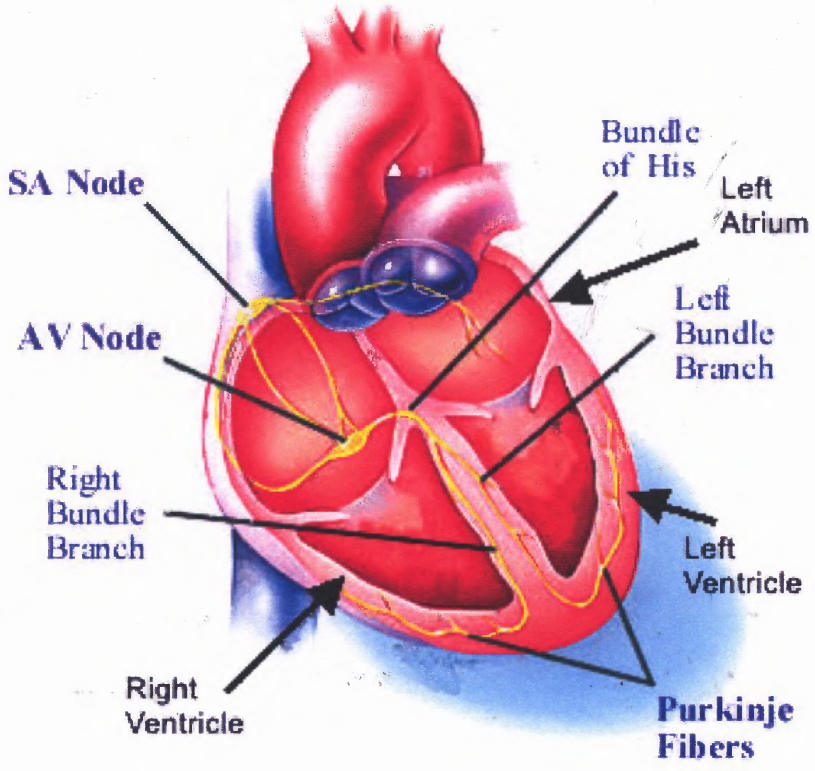

Figure 2.1 Conductive system of the heart [11].

2.1.2 The Normal Electrocardiogram

The normal electrocardiogram (shown in Figure 2.2) is composed of a P wave, a QRS complex and a T wave. The QRS complex can be considered as three separate waves, the Q wave, the R wave and the S wave. The P wave is caused by the electrical potentials generated as the atria depolarize before contraction. The QRS complex is caused by the potentials generated when the ventricles depolarize before contraction. The T wave is caused by potentials generated as the ventricles recover from the state of depolarization. This process occurs in the ventricular muscle 0.25 – 0.35s after depolarization and is know as a repolarization wave. Thus, the electrocardiogram is composed of both depolarization and repolarization waves.

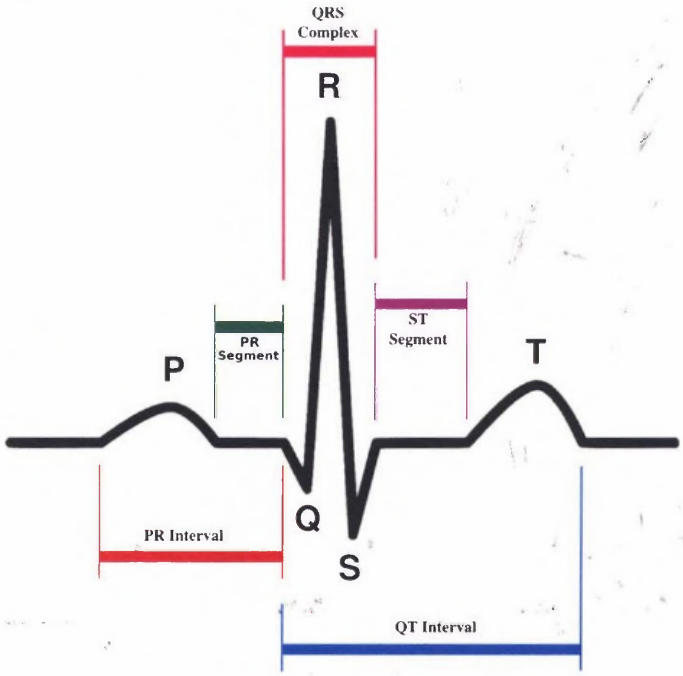

Figure 2.2 Normal ECG waveform [12].

2.1.3 ECG Leads

The ECG is recorded by placing an array of electrodes at specific locations on the body surface (see Figure 2.3). Conventionally, electrodes are placed on each arm and leg, and six electrodes are placed at different locations on the chest. There are three types of ECG leads: standard limb leads, augmented limb leads, and chest leads. These electrode leads are connected to a measurement device that measures the potential difference between the electrodes to produce ECG. The limb leads are referred to as bipolar leads because the trace corresponds to the difference of electrical potentials that exist between two electrodes.

In standard lead I, the positive electrode is placed on the left arm and the negative electrode on the right arm, measuring the potential difference between them. In lead II, the positive electrode is placed on the left leg and negative electrode on the right arm. In lead III, the positive electrode is placed on the left leg and the negative electrode on the left arm. In all lead configurations, the difference of potential measured between two electrodes is always with reference to a third electrode which is placed on the right leg. In defining the bipolar leads, Einthoven postulated that at any given time of the cardiac cycle, the electrical axis of the heart can be represented as a two dimensional vector. The ECG measured from any of the three standard leads is a time-variant single dimensional component of the vector. He proposed that the electric field of the heart could be represented diagrammatically as a triangle, with the heart located at the centre. It was shown that the instantaneous voltage measured from any of the three limb leads is approximately equal to the algebraic sum of the other two.

There are three augmented limb leads. Each of these leads has a single positive electrode which is referenced against a grouping of two other limb electrodes. In the aV_R lead, the right arm is recorded with respect to a reference of a combination of the left arm and left leg electrodes. In the aV_L lead, the left arm is recorded with respect to a reference of a combination of right arm and left leg electrodes. In the aV_F lead, the left leg is recorded with respect to a reference of a combination of the two arm electrodes.

The chest leads are unipolar leads. These six positive electrodes are placed on the surface of the chest where heart is located to record electrical activity in a horizontal arrangement. The six leads are named as V_1 to V_6. These leads are arranged from right of the sternum over the fourth intercostal space laterally towards the left ventricular wall [13].

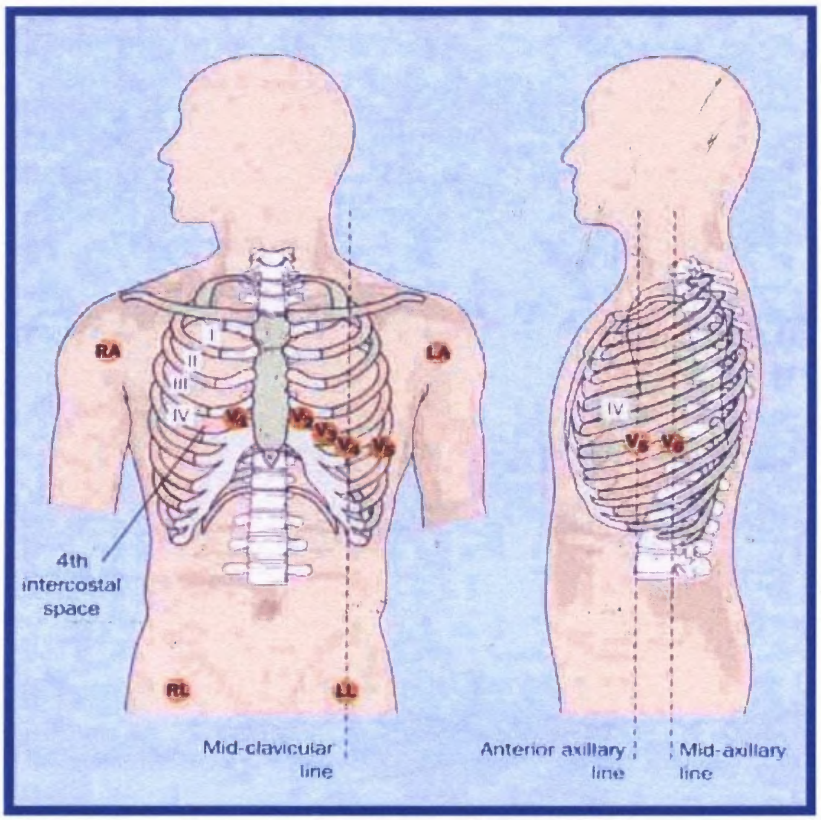

Figure 2.3 ECG lead placement [14].

2.2 Physiology of Respiration

2.2.1 Pulmonary Ventilation

The goal of respiration is to provide oxygen to the tissues and to remove carbon dioxide. Pulmonary ventilation is the phenomena by which the inflow and outflow of air takes place between the atmosphere and the lung alveoli (Figure 2.1.1). Pulmonary ventilation is caused by the muscles of the thorax and diaphragm by creating negative and positive pressures for inspiration and expiration respectively. The lungs can be expanded and contracted in two ways: by increasing and decreasing the chest cavity by downward and upward movement of the diaphragm and by elevation and depression of the ribs to change the volume of the chest cavity [15].

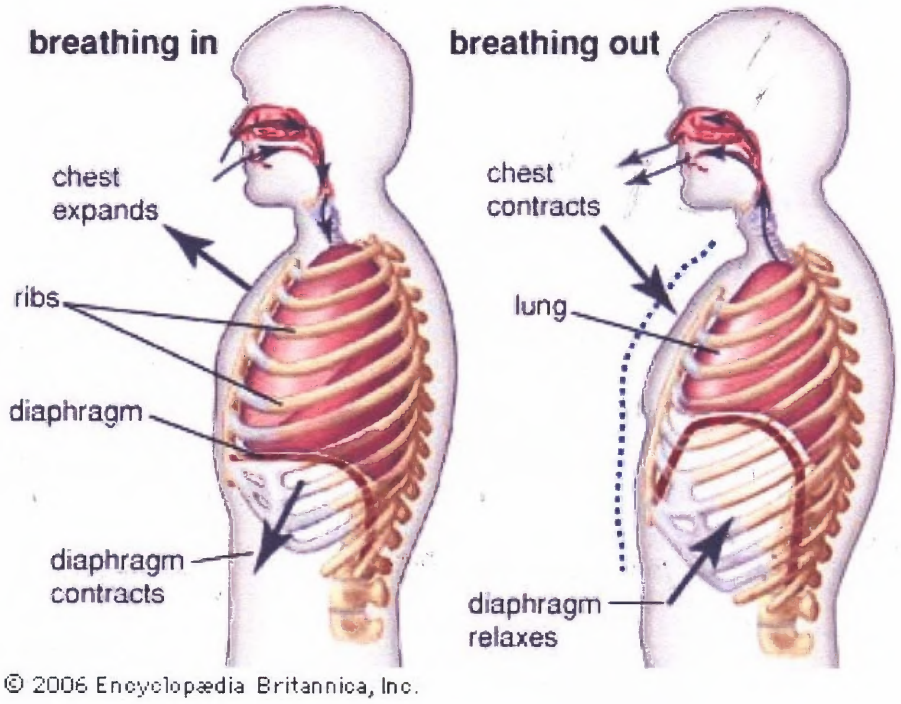

Figure 2.4 Expansion and contraction of thoracic cage during expiration and inspiration [16].

Normal quiet breathing can be carried out completely by the first method i.e., by moving the diaphragm. The contraction of diaphragm pulls the lower part of the lungs downward during inspiration and the relaxation of diaphragm, recoil of the lungs, chest wall and abdominal structures compresses the lungs during expiration. During physical activity when heavy breathing is required the recoiling forces are not sufficient to carry out rapid expiration so extra force is provided by the contraction of abdominal muscles. Another method for expanding the lungs is to raise the rib cage. This causes lungs to expand. Therefore, the muscles that help the lungs to expand by elevating the rib cage are categorized as muscles of inspiration and the muscles that depress the rib cage are categorized as the muscles of expiration [15].

2.2.2 Respiratory Center

The nervous system automatically adjusts the rate of ventilation to meet the demands of the body so that the arterial blood oxygen pressure and carbon dioxide pressure is not altered even during moderate to heavy exercises. The respiratory center is located bilaterally in the medulla oblongata and pons. It is divided into three major regions of neurons: (1) a dorsal respiratory group, which is located in the dorsal portion of the medulla. It mainly controls inspiration. (2) A ventral respiratory group is located in the ventro-lateral part of the medulla. It can cause inspiration or expiration depending on which neurons are excited. (3) The pneumotaxic center is located dorsally in the superior portion of the pons. It helps control the respiration rate and pattern of breathing [15].

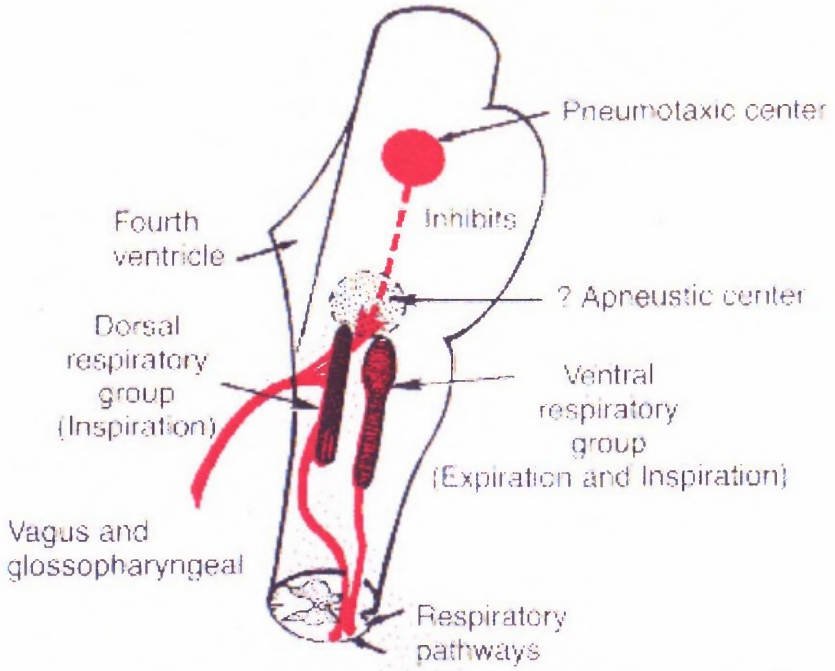

Figure 41–1. Organization of the respiratory center.

Figure 2.5 Organization of the respiratory center [15].

2.2.3 Measurement of Respiration Rate

Under normal circumstances respiration is a rhythmic action, so respiration rate provides clinical information of diagnostic value about the respiratory efforts. Several techniques have been implemented for the measurement of respiration rate.

2.2.3.1 Displacement Method. The respiratory cycle is accompanied by changes in thoracic volume. These changes can be detected by means of a displacement sensor that uses a strain gauge. The sensor is enclosed by an elastic band which is tied around the waist. Respiratory efforts result in resistance changes of the strain gauge connected to an arm of a Wheatstone bridge [10].

Figure 2.6 Displacement sensor for respiration measurement [17].

2.2.3.2 Thermistor Method. Air is warmed when it passes through the lungs and the respiratory tract. This difference in temperature between the inspired and expired air can be detected by a thermistor placed in front of the nostrils by a proper arrangement [18].

Figure 2.7 Thermistor sensor for respiration measurement [19].

2.2.3.3 Impedance Pneumography. This is an indirect method for measuring respiration. External electrodes are applied on the thorax to measure respiration rate using the relation between respiratory depth and thoracic impedance change. It does not require placement of any sensor near the nose and offers minimal hindrance to the patient. This technique uses a high frequency current through the electrodes and detecting the modulated signal. The signal is modulated by the changes in thoracic impedance due to respiratory efforts [18].

2.3 ECG Derived Respiration

2.3.1 Initial Work in ECG Derived Respiration (EDR) at MIT, Cambridge

Moody and his colleagues at MIT Cambridge published a paper in 1985 [1] describing a technique for deriving respiration signal from multi lead ECG. The main advantage of this signal processing technique is that no additional hardware or sensors are required for implementing it. They compared the technique with conventional respiration measurement techniques and showed the derived respiration can be used for consistent detection of central, mixed and obstructive apneas. Additionally, they went on to show that the technique can confidently recognize central and mixed apnea, hypo-apnea, and tachy-apnea.

Their technique was based on the fact that the respiration induces an apparent modulation in the direction of the mean cardiac electrical axis. This is because electrode motion artifact with respect to the position of the heart influences the standard ECG obtained from the body and thereby the electrical impedance of the thorax. For demonstrating the changes in electrical axis due to respiration, they measured the area of QRS complex in two orthogonal leads over a fixed time window which as shown in Figure 2.8 are A_x and A_y. Since the window width is fixed, the area is proportional to the amplitude of the ECG signal, hence to the projection of the mean cardiac electrical vector on the lead axis. When the leads are orthogonal, the arctangent of the ratio of the QRS areas measured in the two leads results in the angle (θ) of the mean axis with respect to one of the lead axes. Then the angle values were interpolated to produce a continuous ECG-derived respiratory signal.

They also suggested that a single lead could be used for deriving respiration signal. Using a single lead ECG, QRS area measurements from that lead can still be used to approximate the respiratory signal and measure respiratory rate. The single lead EDR can produce a relatively large signal, if the lead axis is considerably different from the mean electrical axis. The greatest signal-to-noise ratio is normally obtained when the lead axis is orthogonal to the mean electrical axis, as noise does not change in proportion to the amplitude of the signal.

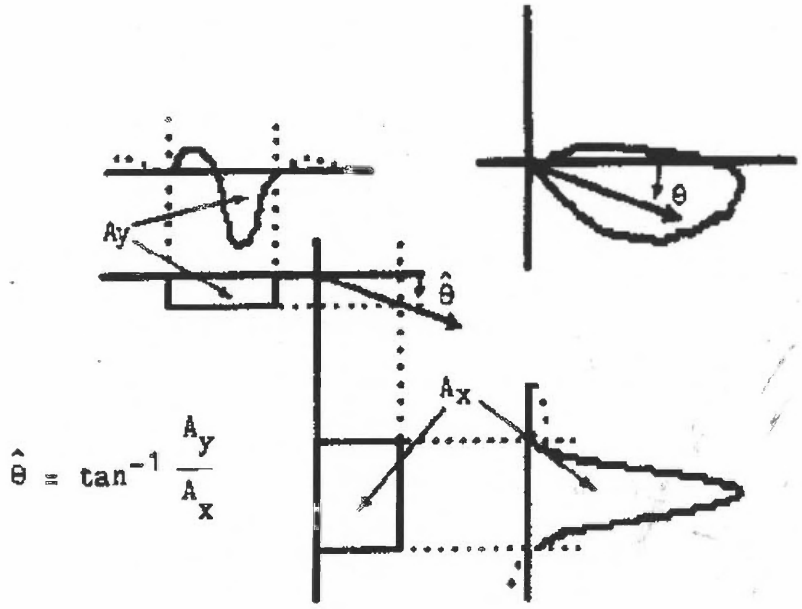

Figure 2.8 Electrical axis measurement technique [1].

2.3.2 EDR by Reisman at NJIT

Based on the electrical axis detection technique, many studies were conducted to implement EDR in different applications. Reisman and his colleagues at NJIT [20] used this multi-lead technique for heart rate variability studies. Their study shows that during inhalation and hold, the amplitude of lead I decreases and that of lead III increases appreciably, while during exhalation and hold, the amplitude of lead I increases and that

of lead III decreases. This observation can be explained by the fact that during inhalation, the lungs are filled with air and diaphragm moves inferiorly, as result of which the apex of the heart is stretches towards the abdomen, while during exhalation the lungs are emptied and diaphragm moves superiorly, which causes the apex of the heart to be compressed towards the chest. This clearly indicates that the respiration causes detectable change in the amplitude of the QRS complex in a single lead ECG.

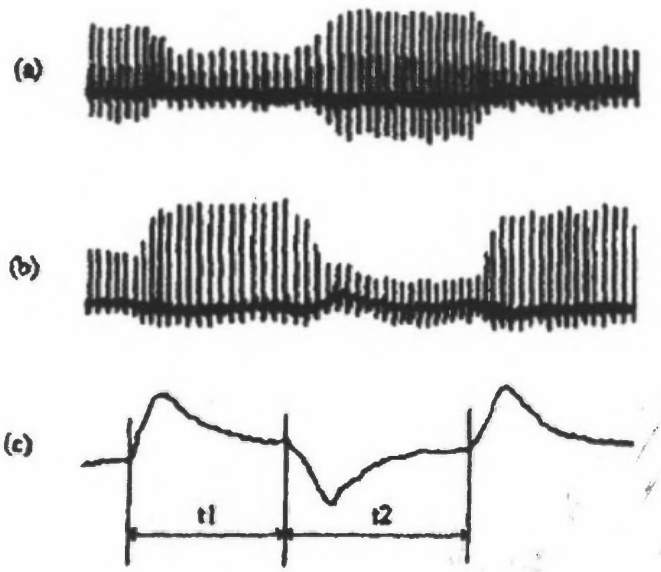

Fig. 1 ECG signals influenced by respiration (a) lead I, (b) lead III, (c) respiration wave

Figure 2.9 ECG signals influenced by respiration [20].
(a) Lead I, (b) Lead III and (c) Respiration wave

Power spectral analysis of heart rate variability is a powerful tool for assessing the neuro-cardiac control mechanism influencing day to day life in clinical conditions. However, in spectral analysis of heart rate variability, the most distinct peak reflects changes in beat to beat interval that oscillates at the same frequency as respiration. Their motivation was to determine the frequency of the spectral peak occurring at the

respiration frequency and thereby ascertain the influence of the respiratory system in heart rate variability (HRV) during stress testing, since it has been observed that the power in the very high frequency band (0.4–1 Hz) has potential application in diagnosis of coronary artery disease.

2.3.3 R Wave Duration based EDR technique for Sleep Analysis

Researchers at Tel Aviv University, Tel-Aviv, Israel derived EDR signal by measuring the R Wave Duration (RWD) [21]. This technique is a different method for measuring the change in QRS area which is the basis for EDR detection. The aim of this study was to quantify the ECG Derived Respiration (EDR) in order to extend the capabilities of ECG based sleep analysis. First they implemented an R wave detection algorithm followed by RWD detection. An algorithm detected local extreme points of the first derivative of the R peak called the inflection points. When a curve changes from concave to convex, a local maximum in the first derivative is called the left inflection point, and when it changes from convex to concave, a local minimum is called the right inflection point. R wave duration (RWD) is defined as the time between these two inflection points adjacent to every R wave peak. The RWD values were plotted against time to get an EDR signal [22].

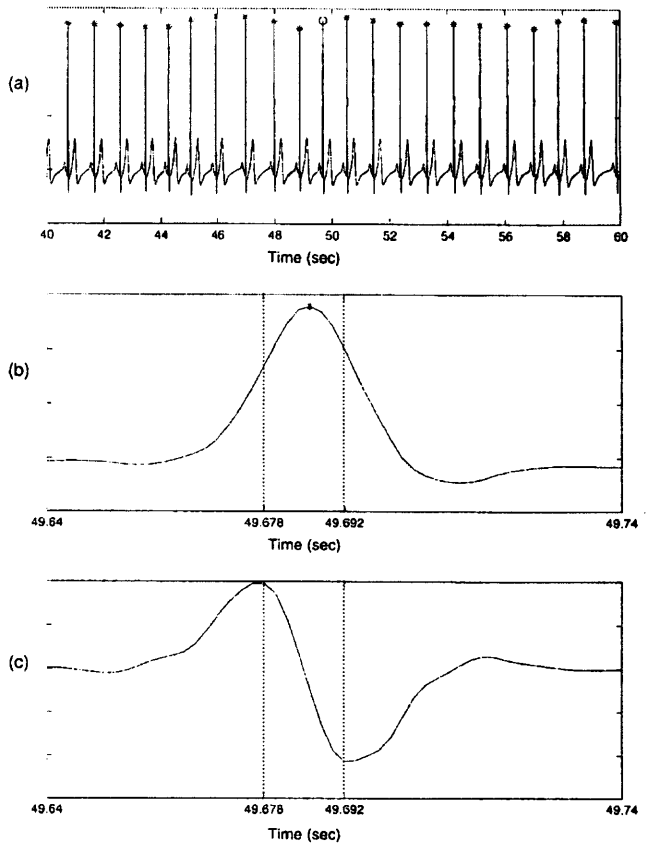

Figure 2.10 R wave duration measurement technique for EDR [22].
(a) ECG, (b) QRS peak and (c) differential of QRS peak

The next step was to implement these single lead techniques in LabVIEW to obtain EDR signals and compare them. To determine the accuracy of these techniques, the derived respiration signal from each technique was compared to actual respiration signal obtained, using displacement sensor.

2.4 LabVIEW - Software Tool

LabVIEW is a graphical programming language. It uses a dataflow programming model that provides an intuitive interface to build design, control, and test applications. The graphical dataflow language and block diagram approach naturally represent the flow of data and intuitively map user interface controls to data, so it is very easy to view and modify data or control inputs, visualize results in graphs and charts, create custom user interfaces and reports in text files, HTML, Microsoft Word, Microsoft Excel, and more.

One of the major advantages of LabVIEW is the relative ease with which one can acquire analog/digital signals from sensors. These acquired signals contain information about a physical quantity of interest. However, the information may not be available directly from the sensors and may require further processing in order to derive useful information. LabVIEW provides an extensive library of functions called VIs (Virtual instruments) to perform different kinds of signal manipulation and processing. For e.g. there are VIs for waveform measurements, waveform monitoring, waveform generation, signal processing and mathematics. With the help of such VIs one can perform different operations on the signal and hence derive the required information without much difficulty [23].

Owing to the extensive signal manipulation functions available, all the algorithms have been implemented in LabVIEW. The data analysis was performed using the 'Probability and Statistics' toolbox of LabVIEW, and the Application Builder module was used to create the executable program, which uses the digital files containing ECG data as an input, and creates the ECG derived respiration rate signal as the output.

2.5 Physiological Data

The physiological data used for this research, was originally obtained for a study of controls and apparently healthy subjects with Presbyopia by Dr. Petrock [24]. All the IRB protocols had been followed during the study which was conducted at the Laboratory for Visual Processes in the Department of Biomedical Engineering at New Jersey Institute of Technology. Continuous Respiration and Electrocardiogram (ECG) were recorded for three different controlled breathing levels: 8 breaths/min, 12 breaths/min, and 16 breaths/min in an effort to obtain respiration rates in the low and high HRV cardiac autonomic response ranges.

The data were collected from 10 subjects, which included presbyopic and control human subjects. The ages of the controls ranged from 18-35. The ages of the presbyopic group ranged from 50 – 75.

ECG and respiration were acquired using a National Instruments DAQ card that obtained analog data from Grass bioamplifiers. The ECG was measured using passive electrodes that were passed to the Grass-Telefactor model IP511, which is an industry standard isolated physiological pre-amplifier. Respiration measurement was done by placing a displacement type Grass-Telefactor respiratory effort transducer around the subject's ribcage. The respiration measurement was obtained by recording the difference in the microvolt amplitude signal that is generated when the piezo film is stretched or compressed due to the exhalation or inhalation respectively.

The subject was asked to focus on a green light which blinked at frequencies of 8, 12 and 16 per minute to obtain paced breathing rates. The DAQ acquired the physiological signals at a rate of 500 samples/sec to ensure frequency resolution.

In addition to the paced breathed data, to demonstrate the use of the developed technique in producing a respiration rate signal from raw ECG, few samples of stress data that included exercise and recovery periods were obtained form Dr Zaim [25]. The exercise data had been originally obtained for a study by Dr. P. Asselin at University of Medicine and Dentistry, Medical School, Newark [26].

CHAPTER 3

IMPLEMENTATION OF ALGORITHMS FOR ECG DERIVED RESPIRATION RATE

3.1 Algorithm for R Wave Detection

The algorithms for deriving respiration from ECG need indices of R wave locations. Therefore, an accurate means of detecting all the R waves is needed. ECG signals were passed through an R wave detection algorithm [26] developed at NJIT several years ago, using LabVIEW. The resulting array of R wave indices was used to derive the necessary respiratory information. The figure 3.1 depicts the block diagram of the R wave detection algorithm.

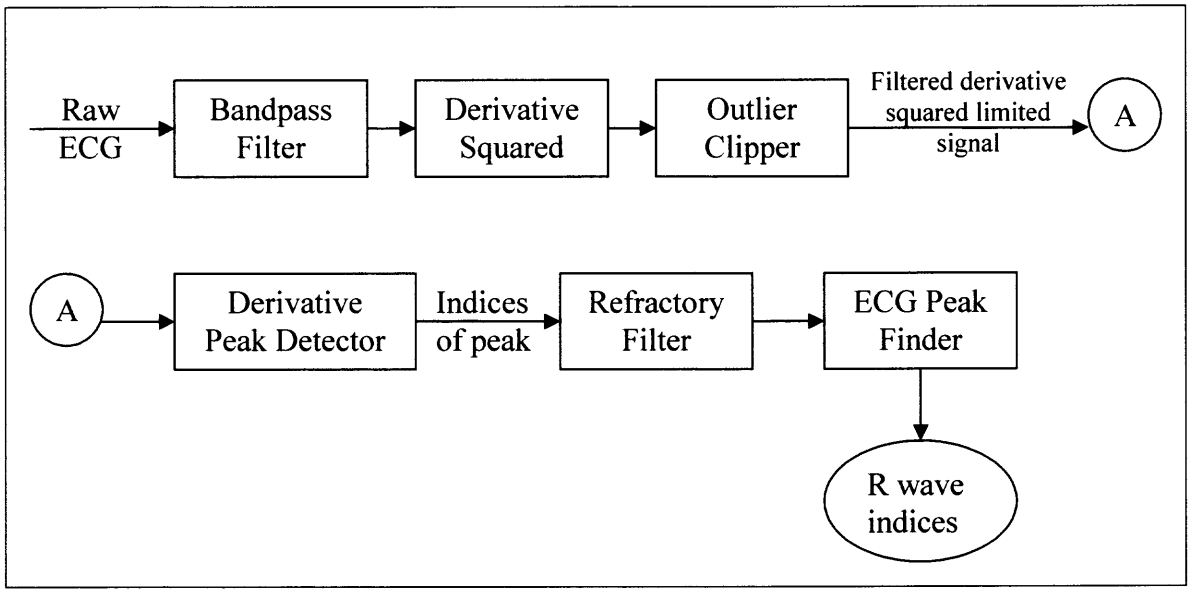

Figure 3.1 Block diagram of R wave detector algorithm.

The raw ECG is first passed through a Butterworth bandpass filter with a higher cutoff frequency of 40Hz and a lower cutoff frequency of 0.5Hz. The higher cutoff frequency removes unwanted high frequencies that may be present due to muscle activity

and the lower cutoff frequency ensures stability of baseline. The filtered signal is passed through a series of subroutines which detect the indices of QRS peaks in the signal. Since peaks are features of the waveform which have high slopes, the first derivative is calculated and then squared to remove negative values. As a result of derivative function the peaks are enhanced. However, this process also enhances the high frequency noise. For removing the unwanted noise peaks which may have been detected as an R wave peak, the signal is passed through an outlier clipper. This filter clips away all very high amplitude noise peaks. The derivative squared limited signal is then passed through a simple peak detector, where the amplitude of each point is compared to the threshold of 30% of maximum valued point in the segment. The resulting array gives indices of peaks from the filtered derivative squared limited ECG signal.

The ECG is a complex signal consisting of various features which requires the peak detector to make special considerations for locating the peaks. The T wave which immediately follows the R wave also has a prominent peak which is likely to be detected as a QRS peak. A refractory filter is added to remove any peak which falls within a refractory period of 200ms after a QRS peak has been detected. Thus obtained are indices of peaks in the derivative squared ECG, which can be used to locate the peaks in the actual filtered ECG. The peak finder block finds maximum value from the filtered ECG within a period of +/-60ms of maximum derivative point regardless of sampling rate. This strategy is based on the width of R wave, as the maximum is before R wave or between the R and the S waves. The peak finder generates an array of indices of QRS peaks in actual ECG.

The robustness of the R wave detection algorithm can be observed in the noisy segment of ECG shown in Figure 3.2.

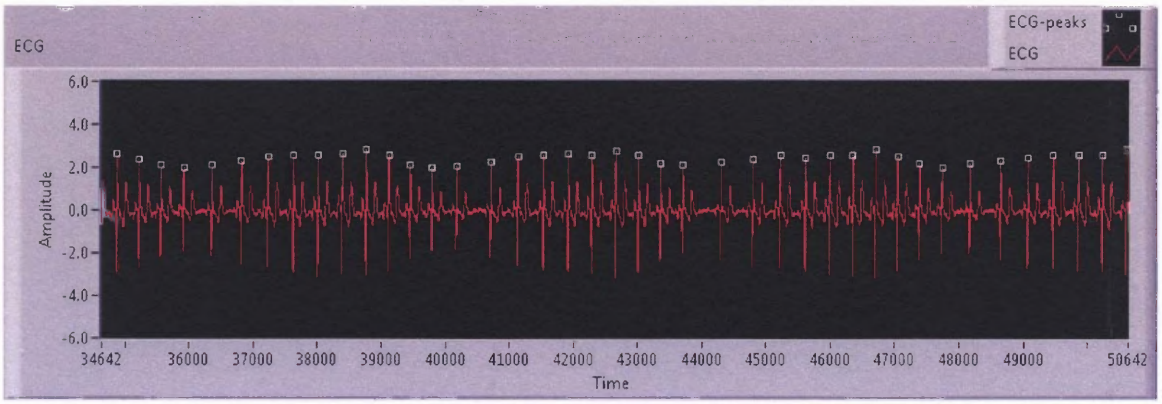

Figure 3.2 ECG marked with QRS peaks.

3.2 Methods for EDR

Based on researching different EDR detection techniques, two promising methods were studied in order to find the better method for deriving respiratory information from a single lead ECG. Also a third method was developed to take advantage of respiration features from both the methods. The three methods studied are:

1. R wave amplitude modulation technique (RWA)
2. R wave duration measurement technique (RWD)
3. Product of RWA and RWD

3.2.1 RWA

The array of indices of QRS peaks generated by the R wave detection algorithm from the given ECG waveform can be used for obtaining respiration information. Lead I ECG signals were used for the study. As shown by Reisman [210], during inhalation and hold, the amplitude of lead I decreases, while during exhalation and hold, the amplitude of lead

I increases. R waves being the high amplitude features of the ECG experience maximum modulation by the respiratory efforts. The peaks of R waves, i.e., QRS peaks depict the change in amplitude caused by respiration. Thus the R wave amplitude modulation effect can be used to obtain ECG derived respiration (EDR).

The modulating signal was obtained by using the indices of QRS peaks to obtain the amplitude of those peaks. The peak amplitudes thus obtained represent the modulating signal, which is the respiration signal. However, the peaks form a discontinuous signal which is not a proper representation of the respiration signal. To obtain a continuous time sampled waveform, the peak array was passed through a spline interpolator which inserted points between the unevenly distributed peaks to obtain a continuous time varying waveform.

During data acquisition actual respiration signals were obtained by Dr. Petrock [24] using a displacement sensor simultaneously with the ECG. Therefore, the effectiveness of EDR algorithm and the resulting respiration signal could be compared with the actual respiration signal from the same patient (see Figure 3.3). The two waveforms, derived (red trace) and actual (white trace), appear to be similar, and subsequent analysis will determine the similarity. Note that the goal of developing the EDR signal is not to reproduce an exact respiration signal, but rather to produce an accurate measure of the respiration rate.

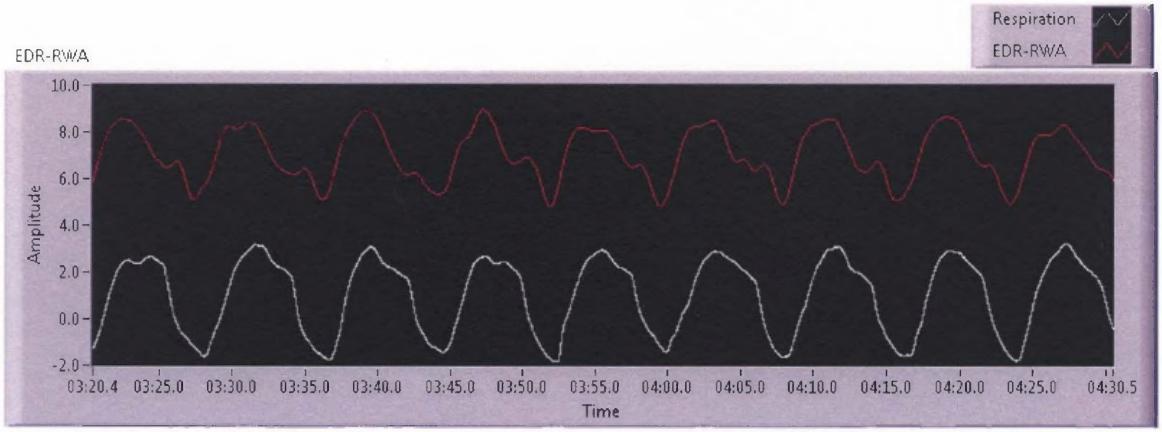

Figure 3.3 Actual respiration and respiration derived using RWA technique.

3.2.2 RWD

Respiration causes a change in the area under the R wave and this is the basis of using R wave duration measurement for EDR detection [21]. As discussed in the literature search section 2.3.3 the RWD finds the difference between local inflection points. To measure R wave duration, the index of the R wave was used to pass a 40 ms window of ECG derivative signal within +/-20ms of the QRS peak. The local maximum in the first derivative called the left inflection point is a peak and obtained by passing the segment through a peak detector. The local minimum in the first derivative called the right inflection point is a valley and obtained by passing the segment through a valley detector. The local maxima and minima are shown in Figure 3.4. The difference between the indices of the left and right inflection points gives R wave duration. The R wave durations (RWDs) represent the QRS area (see Figure 3.5) which has been modulated by the respiratory efforts. These time difference values when plotted against R wave indices produce a respiration signal. A comparison of the actual (white trace) and derived RWD (red trace) is shown in Figure 3.6.

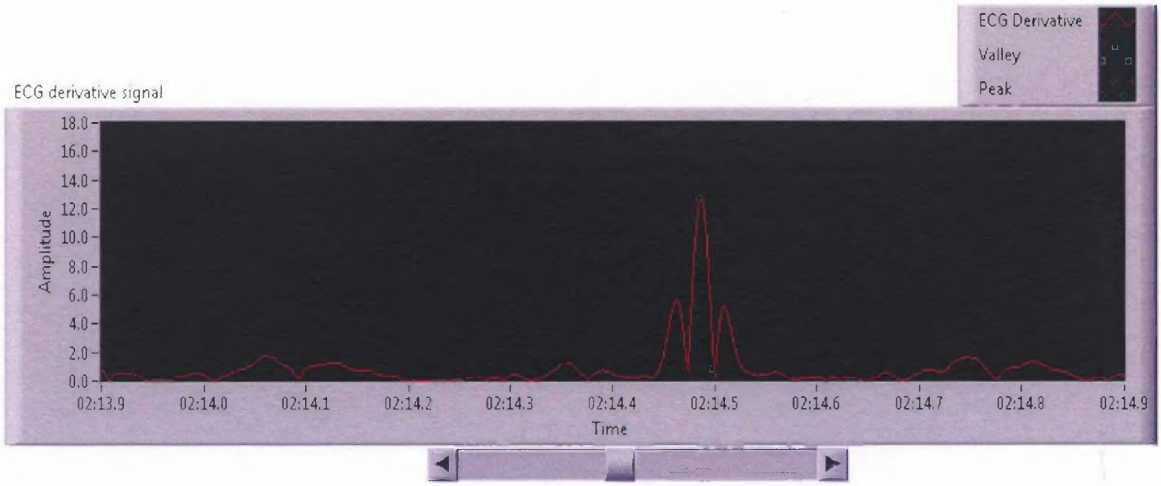

Figure 3.4 A segment with the left and right inflection points on the ECG derivative signal.

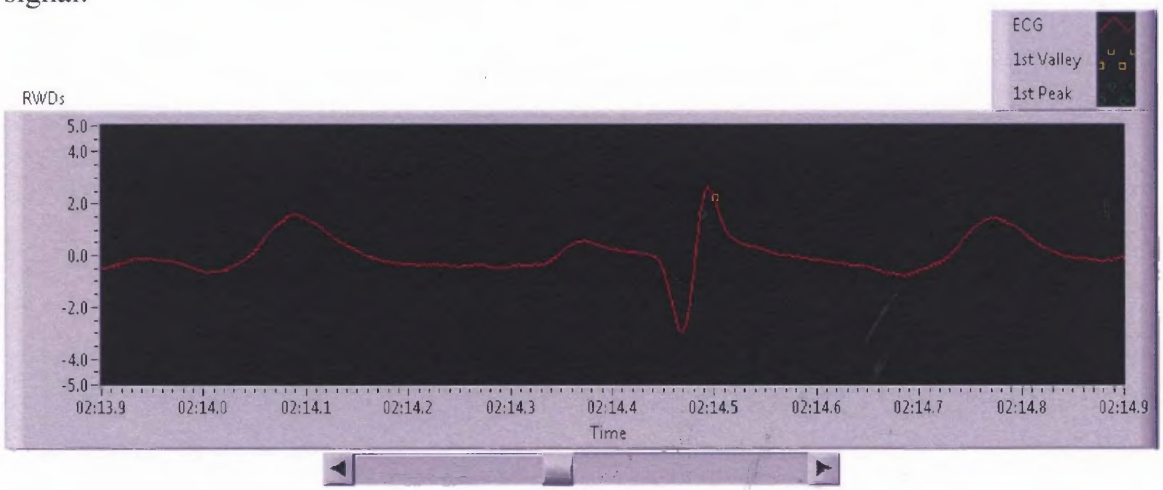

Figure 3.5 A segment with the left and right inflection points on the ECG signal.

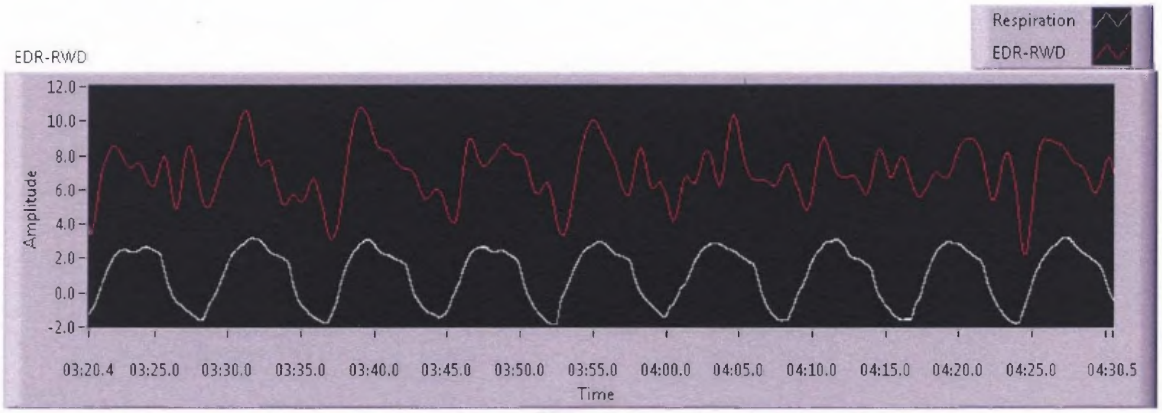

Figure 3.6 Actual respiration and respiration derived using RWD technique.

3.2.3 RWA*RWD

A third method is implemented to combine the respiration information from both the RWA and RWD methods. Point by point product of respiration derived using RWA and RWD methods was calculated to obtain a respiration signal. Figure 3.7 shows the derived respiration signal using this method. The waveform is a modulation of the RWA derived respiration signal by RWD derived respiration. Data analysis will reveal the advantage of this method over another method.

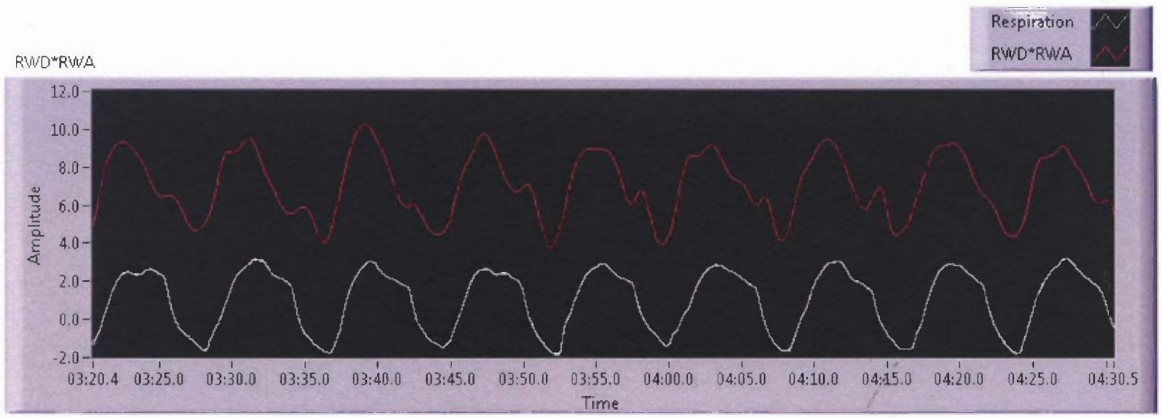

Figure 3.7 Actual respiration and respiration derived using RWA*RWD technique.

3.3 Respiration Rate Signal Extractor Algorithm

In order to validate the effectiveness of the three methods for EDR the derived signal was compared with the actual respiration signal, which was acquired simultaneously with ECG during data acquisition. Data analysis (Section 4.1) revealed that RWA is a superior technique for deriving respiration from single lead ECG and exhibits a high correlation with actual respiration signal. Once respiration signals from both actual and derived methods were available, the goal was to develop an algorithm for obtaining a continuous respiration rate signal. Respiration rate signals can thus be obtained and compared.

A point by point continuous respiratory rate signal can be obtaining by detecting the peaks in the respiration signal. Time between two peaks gives the time period T and 1/T gives the frequency f, of the signal at every peak of the signal. Figure 3.8 depicts the algorithm used in calculating the respiration rate signal for the derived respiration signal. The algorithm consists of a bandpass filter, a two-stage peak detector, a refractory filter to remove unwanted peaks, a peak detector to insert missed peaks, and a spline interpolator to construct the continuous respiratory rate signal.

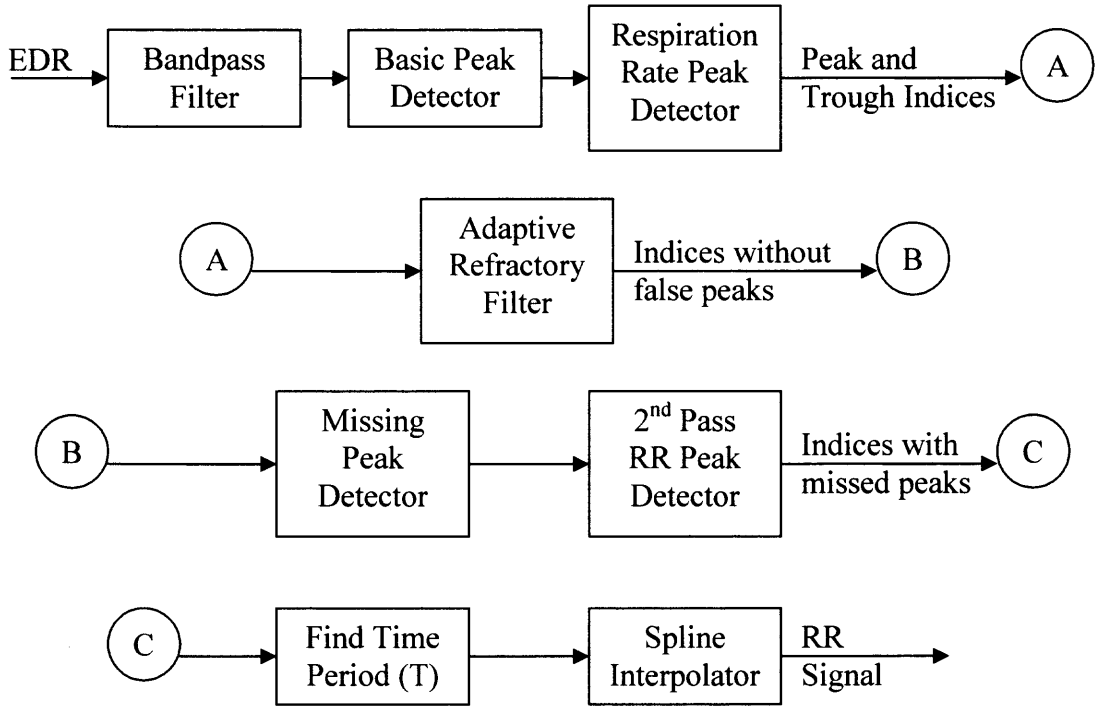

Figure 3.8 Respiration rate signal extractor algorithm.

3.3.1 Bandpass Filter and Respiration Rate Peak Detector

The normal respiration rate ranges from about a few breaths/min to 35 breaths/min. This means that the respiration signal lies in a band of 0.1 to 0.6Hz. A Butterworth bandpass filter with the indicated range is used to filter out the unwanted low and high frequency components of ECG, which are still present in the EDR signal. Cyclical variations existing in the respiration waveform can be detected to measure the respiration rate. However, cyclical variations in the respiration waveform can also be caused by the beating of the heart. These unwanted variations called heart-bumps are difficult to detect and often can be mistaken for respiration features. Franks et al. [27] developed an algorithm for removing heart-bumps. An adaptation of this algorithm is used for removing such features from EDR waveforms.

After passing through the bandpass filter, the respiration waveform is processed by a basic peak detector that detects all the peaks. The detected peaks may be due to the respiratory efforts or due to the heart. As shown in Figure 3.9, the respiration rate peak detector algorithm detects both peaks and troughs. A trough is declared between two peaks if, 1) the amplitude of the negative going portion of the segment (i.e., amplitude difference between peak N and the trough point) is greater than a predetermined threshold value and 2) the positive going portion of the segment (i.e., amplitude difference between the trough point and peak N+1) is greater than a predetermined threshold. Fifty percent of the waveform's root means square (rms) value is taken as the threshold. If a trough is not found in the segment between peaks N and N+1, the algorithm then checks the segment between peak N and Peak N+2. This process

continues till a valid trough and peak pair is found and ensures that a heart-bump is not detected as a breath.

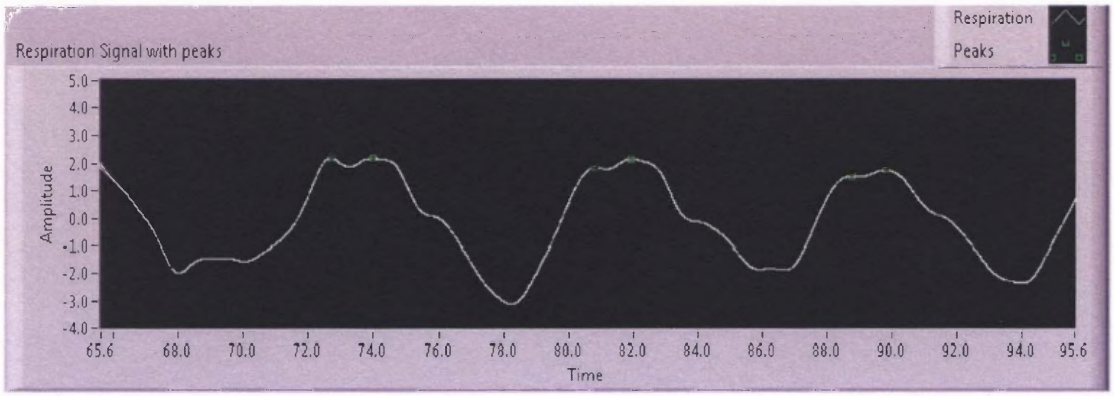

Figure 3.9 Peaks detected by the basic peak detector.

3.3.2 Adaptive Refractory Filter

Other kinds of cyclical variations may also be present in the respiration waveform due to body motion [27]. These can cause large variations in amplitude and may be detected as a breath. To remove these false peaks, a refractory filter is implemented. It removes any peak or trough that occurs too soon. The filter determines a hold-off (refractory) period during which any detected peaks are ignored. The length of the refractory period is adaptive in that it uses 35% of the average of last three inter-breath intervals. If a peak falls before the hold-off, it is removed. When respiration rate is increasing, the inter-breath interval would decrease and so the refractory period is also decreased. Figure 3.10 shows the false peaks that exist before passing through the refractory filter and the same removed after passing through the filter. This adaptive nature of the refractory filter is desirable since the respiration rate signal will be calculated for cases where the ECG was taken during stress tests.

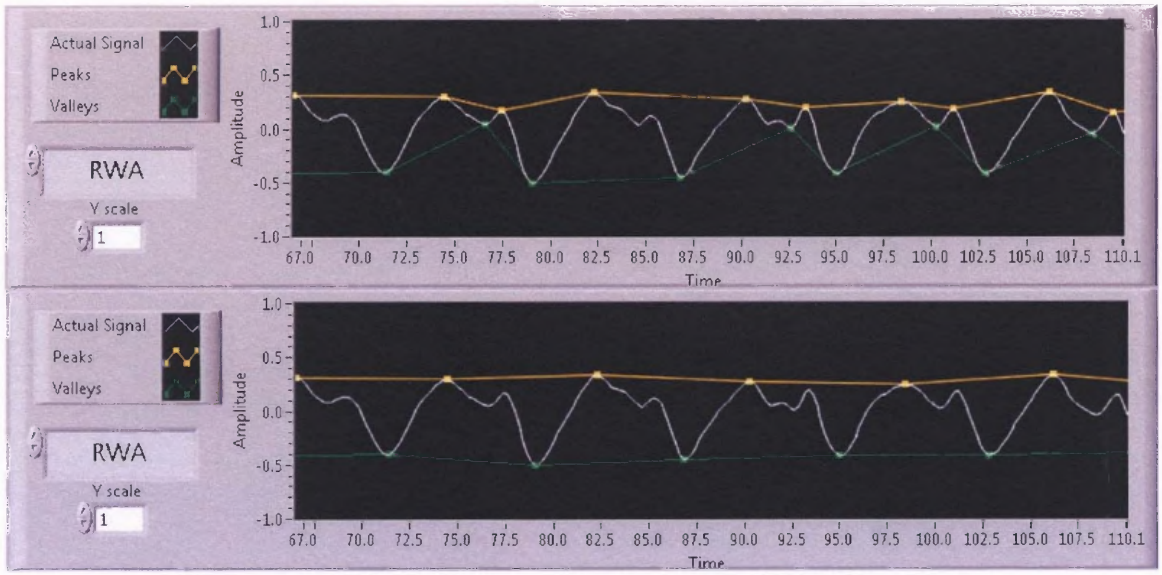

Figure 3.10 EDR-RWA waveform with refractory filter off (top) and on (bottom).

3.3.3 Missing Peak Detector

Refractory filter accounts for peaks that occur too soon, but there are conditions when a peak is detected too late. It is possible that a peak may have been missed in between. To account for such missed peaks, a missing peak detector has been implemented. If a peak does not occur within a time frame of almost two breaths, it is possible that a peak has been missed. Thus the detector indicates a missed peak, if the inter-breath interval for a peak exceeds the average of the last three inter-breath intervals by 75%. Taking the average of the last three inter-breath intervals, makes the detector adaptive and as discussed earlier helps account for changes in respiration rate.

A second pass of the respiration rate peak detector occurs when a peak has been suspected missing. Since the respiration rate peak detector relies on peak-to-trough and trough-to-peak amplitudes being greater than the threshold, a missed peak may be due to the fact that the waveform may have been attenuated due to noise and, thereby, the peak-to-trough and the tough-to-peak amplitudes were less than the threshold level. To find

such peaks and troughs, the threshold is reduced and the peak detection is repeated by the respiration rate peak detector. The top plot in Figure 3.11 shows the missed peak while the bottom plot shows the same peak detected after undergoing a second pass of peak detection.

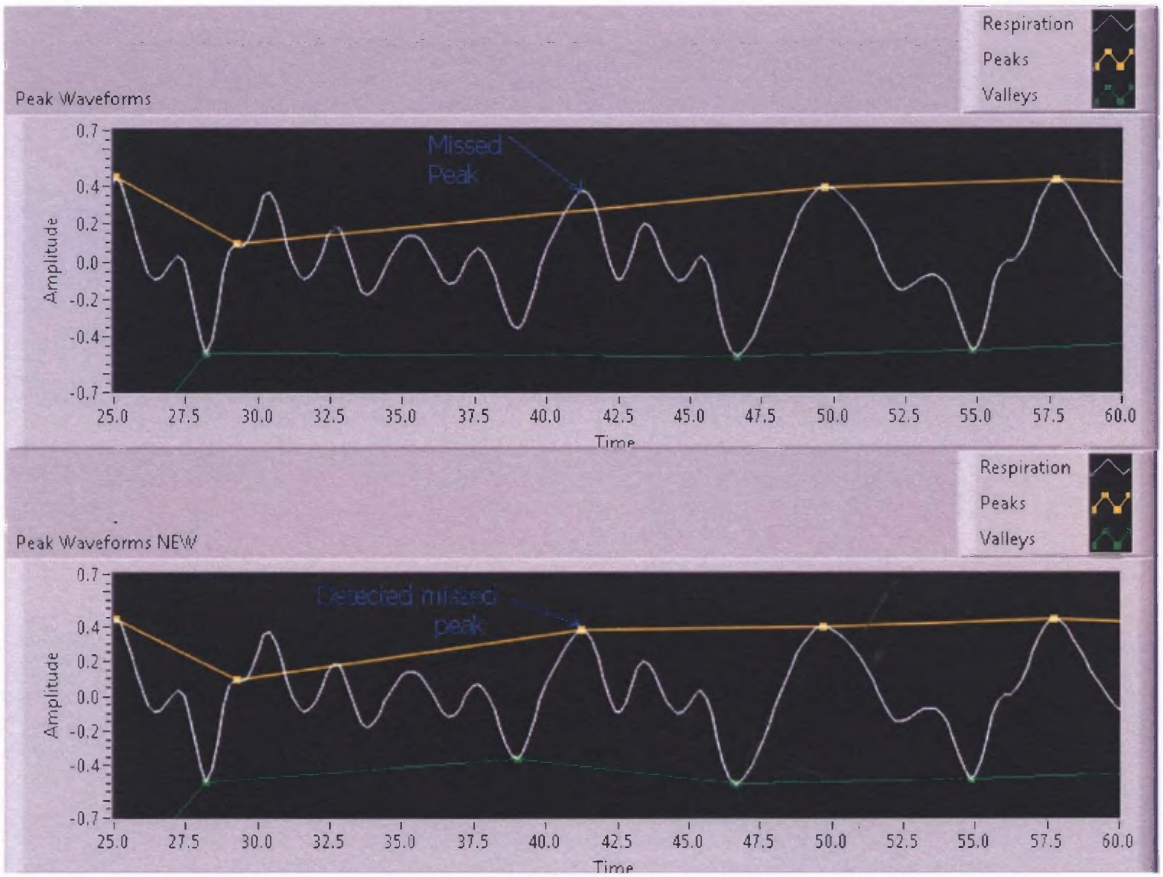

Figure 3.11 EDR segment with a missed peak (top) and after passing through missing peak detector (bottom).

The peak detector algorithm produces the time indices associated with when respiration peaks occur. However, the peaks are not equally spaced in time. To obtain a continuous time sampled waveform, the peak time indices are passed through a spline interpolator to obtain a continuous time varying waveform.

CHAPTER 4

RESULTS

4.1 Viability of EDR Methods

ECG derived respiration signals were obtained using the three methods i.e., RWA, RWD and RWA*RWD. Visual inspection showed good similarity between the derived signals and actual respiration signal. Figures 4.1 a, b, and c shows the different EDR methods plotted against the actual respiration signal with an offset. RWA signals (Figure 4.1(a)) and RWA*RWD signals (Figure 4.1(c)) showed better similarity to the actual respiration signal than the RWD signal (Figure 4.1(b)).

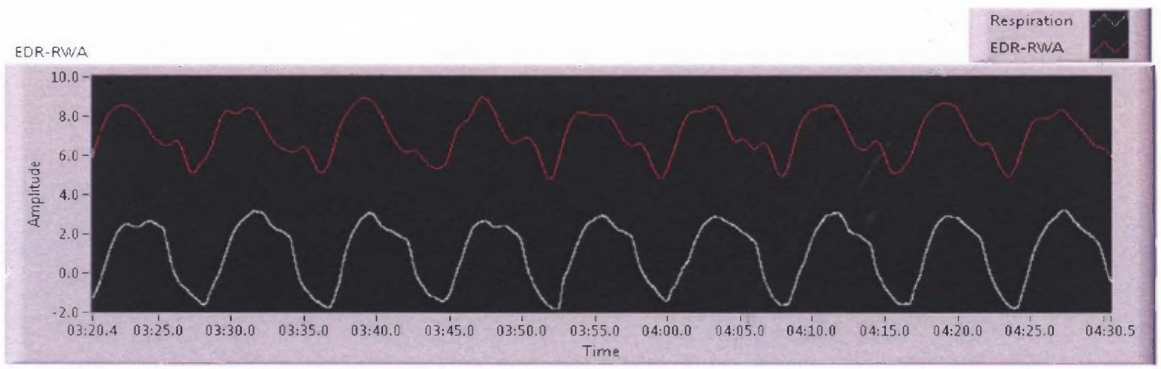

Figure 4.1 (a) EDR signals due to the RWA method plotted against actual respiration.

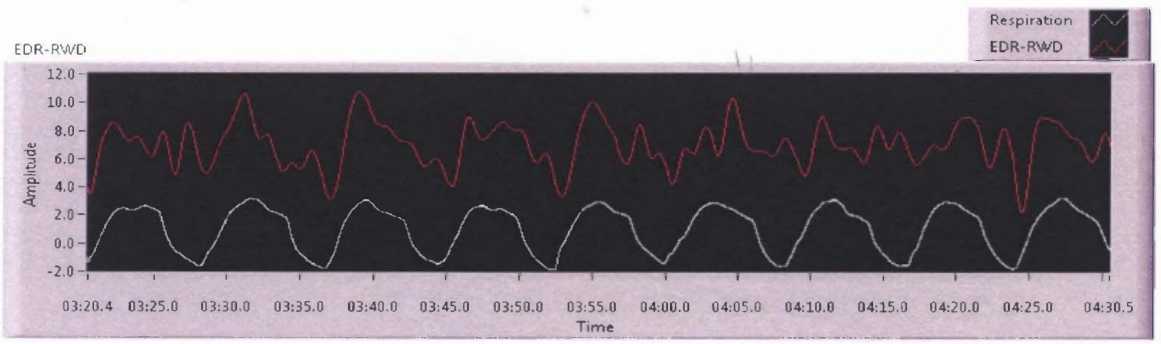

Figure 4.1 (b) EDR signals due to the RWD method plotted against actual respiration.

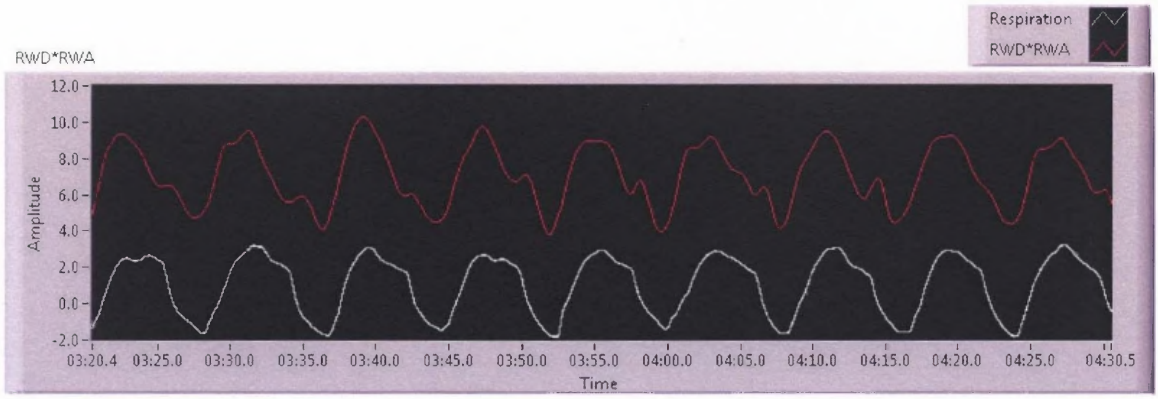

Figure 4.1 (c) EDR signals due to the RWA*RWD method plotted against actual respiration.

The ECG and actual respiration were obtained by paced breathing at 8, 12 and 16 breaths/min; therefore a single frequency would represent the respiratory frequency in the actual as well as the derived respiration signals. Spectral analysis can thus be used to find the respiration frequency and compare the actual and derived signals. To find this respiration frequency, power spectrum is computed using the following equation:

$$PowerSpectrum = \frac{FFT^{*}(Signal) \times FFT(Signal)}{N^{2}} \qquad (4.1)$$

N is the number of points in the signal array and * denotes complex conjugate. In the power spectrum the frequency with maximum power represents the respiration frequency and thus the respiration rate. Figure 4.2 shows the power spectrum of actual respiration and EDR signals along with the estimated frequency peak and respiration rate for a subject, utilizing a LabVIEW program.

Similarly, respiratory rates for all the samples were computed using the power spectrum for quantitative analysis. Tables 4.1, 4.2, 4.3 shows respiration data at different paced breathing rates for actual respiration and EDR signals for different subjects.

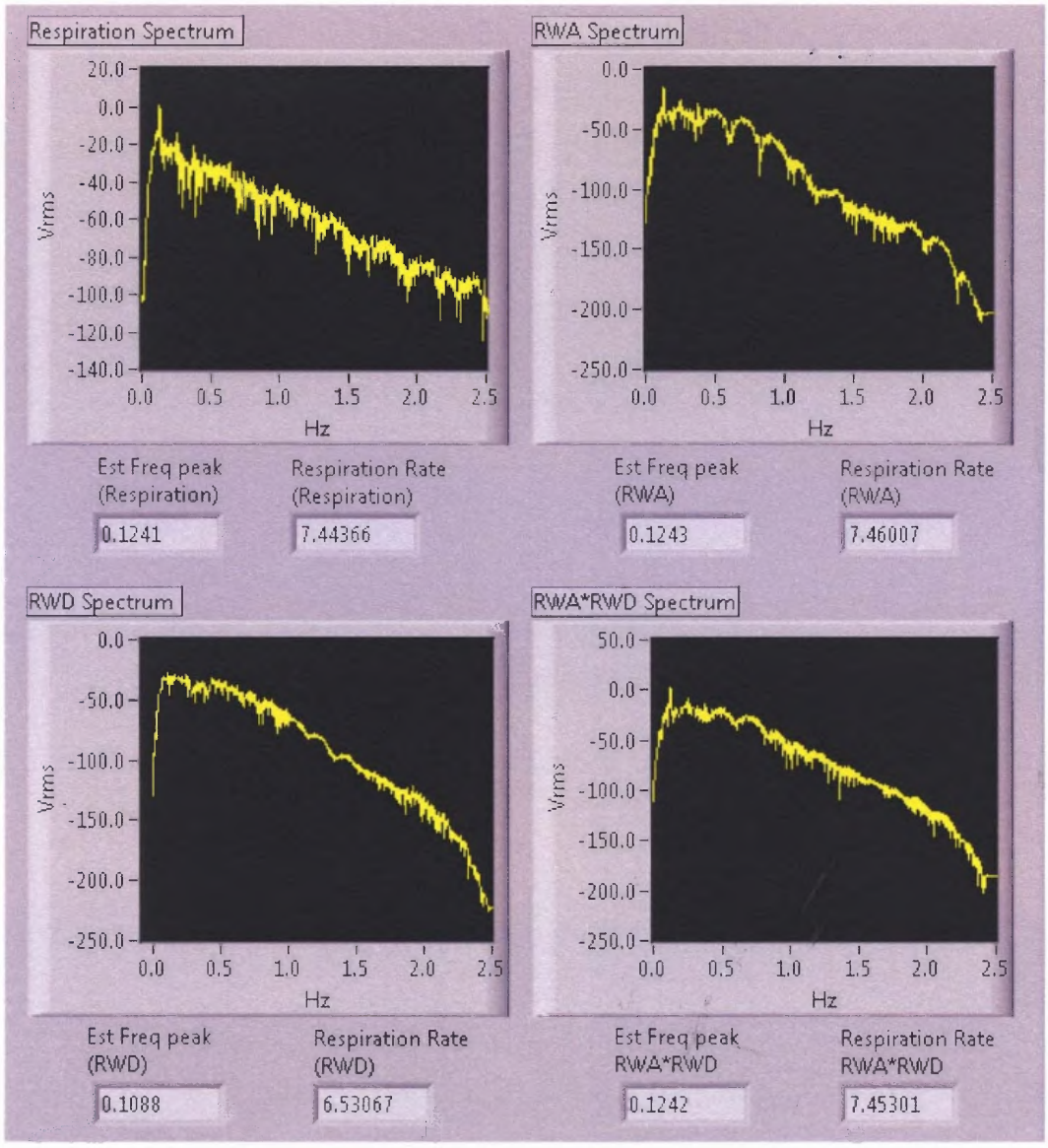

Figure 4.2 Power spectrum of a subject's actual respiration and the three methods of obtaining an EDR signal.

To compare the three EDR techniques with the actual respiration, the mean and standard deviation (SD) for all were calculated and are displayed in the Tables 4.1, 4.2, and 4.3 for each group of paced breathed data. If many data points are close to the mean, then the standard deviation is small; if many data points are far from the mean, then the

standard deviation is large. If all the data values are equal, then the standard deviation is zero [28].

Table 4.1 Respiration Rates for 8 Breaths/min Paced Breathed Samples

Subject	Actual Respiration	RWA	RWD	RWA* RWD
1A	7.522	7.406	6.840	7.389
1B	7.512	7.492	12.088	12.058
1C	7.518	7.495	26.216	9.302
2A	7.465	7.467	7.463	7.460
2B	7.500	7.510	7.535	7.514
3A	7.507	7.498	13.030	7.495
3B	7.472	7.471	7.408	7.466
4A	7.527	7.493	15.850	7.493
4B	7.508	7.507	6.477	7.537
5A	7.497	7.484	7.466	7.485
5B	7.485	7.510	7.483	7.503
6	7.495	7.508	7.435	7.509
7A	7.458	7.449	27.591	7.454
7B	7.502	7.495	7.677	7.497
8	7.492	7.493	7.543	7.479
9A	7.500	7.511	32.160	7.502
9B	7.474	7.481	7.520	7.479
Mean	7.496	7.486	12.222	7.860
SD	0.020	0.027	8.313	1.168

Note: All units are in breaths/min

Table 4.2 Respiration Rates for 12 Breaths/min Paced Breathed Samples

Subject	Actual Respiration	RWA	RWD	RWA* RWD
1A	10.702	10.656	10.725	10.681
2A	10.691	10.773	12.680	12.651
2B	10.677	10.671	10.689	10.675
2C	10.690	10.685	10.678	10.679
3A	10.673	10.663	14.794	10.655
3B	10.690	10.700	17.968	10.697
4A	10.855	10.793	10.077	10.622
4B	10.649	10.652	10.635	10.651
5A	10.728	10.751	19.030	10.748
5B	10.742	10.758	17.224	10.762
6A	10.712	10.726	10.757	10.728
6B	10.686	10.689	10.674	10.686
7	10.693	10.691	8.166	10.695
8A	11.534	11.536	26.363	11.530
8B	11.301	11.276	33.683	11.299
9A	10.635	10.634	10.686	10.632
10A	10.705	10.715	10.792	10.712
10B	10.701	10.712	10.836	10.710
Mean	10.781	10.782	14.248	10.710
SD	0.239	0.235	6.594	0.503

Note: All units are in breaths/min

Table 4.3 Respiration Rates for 16 Breaths/min Paced Breathed Samples

Subject	Actual Respiration	RWA	RWD	RWA* RWD
1A	13.414	13.381	13.424	13.387
1B	13.693	13.708	12.476	12.552
2A	13.626	13.626	13.617	13.623
2B	13.632	13.639	13.631	13.633
3A	13.675	13.671	8.860	13.672
3B	13.626	13.628	13.782	13.625
4	13.636	13.651	13.724	13.687
5A	13.266	13.598	7.502	13.602
5B	13.582	13.556	13.604	13.518
6A	13.602	13.607	13.610	13.607
6B	13.638	13.644	13.652	13.646
7	13.679	13.675	13.804	13.678
8	14.234	14.223	24.674	14.200
9	13.655	13.662	13.132	13.647
10A	13.642	13.634	13.622	13.636
10B	13.665	13.66	13.735	13.661
Mean	13.641	13.660	13.553	13.585
SD	0.192	0.167	3.501	0.320

Note: All units are in breaths/min

Table 4.4 summarizes the results. From this table, for each of the 3 respiration rates, the mean and standard deviation for EDR method using RWA is closest to the actual respiration than the RWA*RWD and RWD methods. This implies that to derive the respiration signal from ECG the EDR method using RWA yields the better fit to the actual respiration than the other two methods.

Table 4.4 Summary of the Mean and SD for All Samples' Respiration Rates

Statistic	Actual Respiration	RWA	RWD	RWA* RWD
Respiration 8 breaths/min				
Mean	7.496	7.486	12.222	7.860
SD	0.020	0.027	8.313	1.168
Respiration 12 breaths/min				
Mean	10.781	10.782	14.248	10.710
SD	0.239	0.235	6.594	0.503
Respiration 16 breaths/min				
Mean	13.641	13.660	13.553	13.585
SD	0.192	0.167	3.501	0.320

Note: All units are in breaths/min

Correlation indicates the strength and direction of a linear relationship between two random variables [29]. In the current research actual respiration and derived respiration are the two random variables to be compared. RWA gives a correlation of 0.945 with actual respiration while RWD and RWA*RWD give correlation of 0.066 and 0.757 respectively. Correlation analysis also points that RWA is a better estimator of respiration signal than the other two methods.

The scatter plot is also considered a good technique for comparison of a new measurement technique with an established one [30]. For the current research it is necessary to determine whether the displacement sensor and EDR techniques for obtaining respiration signal agree sufficiently and if the derived signal can replace the actual signal. When the data is plotted, all points would lie on the line of equality, if the two techniques exhibit perfect agreement. Figure 4.3 shows the scatter plots for comparing displacement sensor technique with EDR techniques for obtaining respiration signal. It is clear that the respiration signal obtained using RWA is in good agreement with the actual respiration.

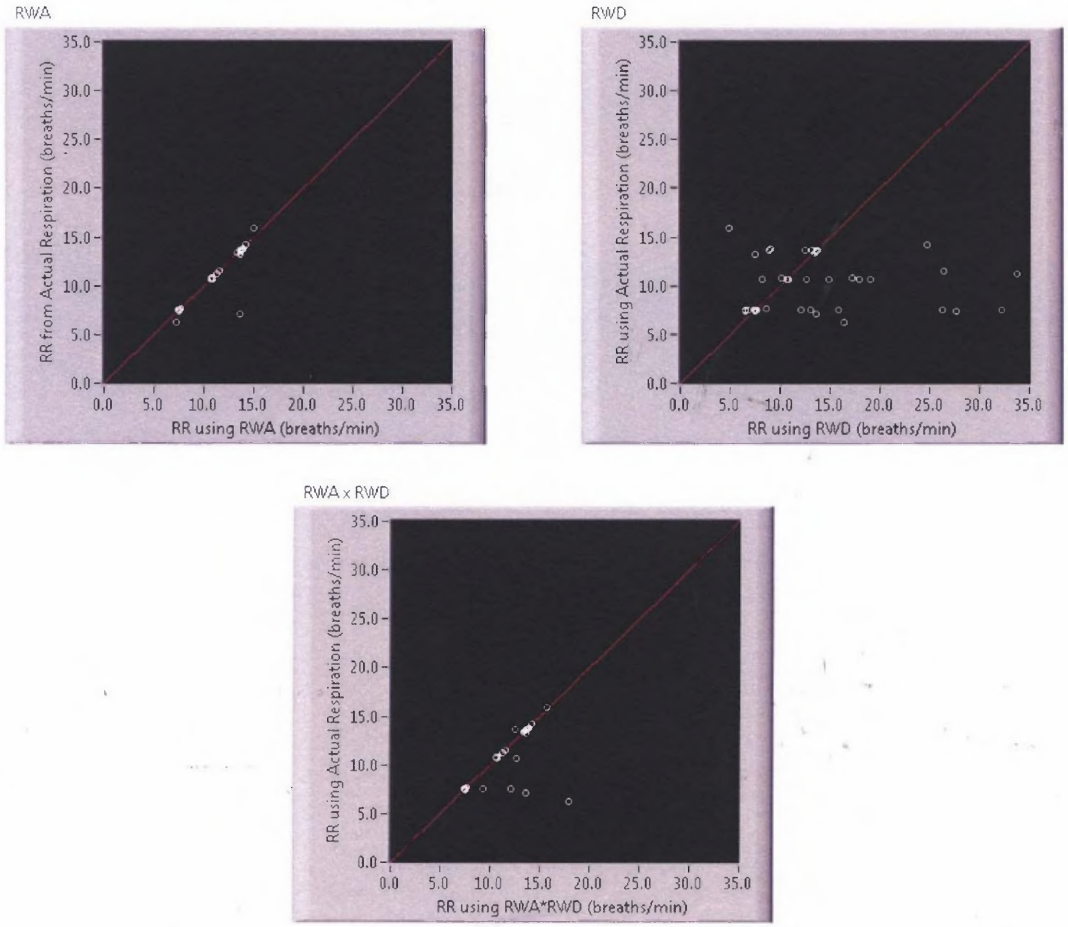

Figure 4.3 Scatter plots for comparing displacement technique with EDR techniques for obtaining respiration signal.

4.2. Viability of Respiration Rate Algorithm

Data analysis of EDR signals by spectral analysis, correlation coefficients and scatter plots reveals that RWA is a preferable method for deriving respiration from a single lead ECG. Once the best technique was identified, an adaptive algorithm was developed to obtain a continuous respiration rate signal. Figure 4.4 shows respiration rate signal obtained from both the actual respiration and derived one using RWA technique. Visual inspection shows that both signal show a degree of similarity.

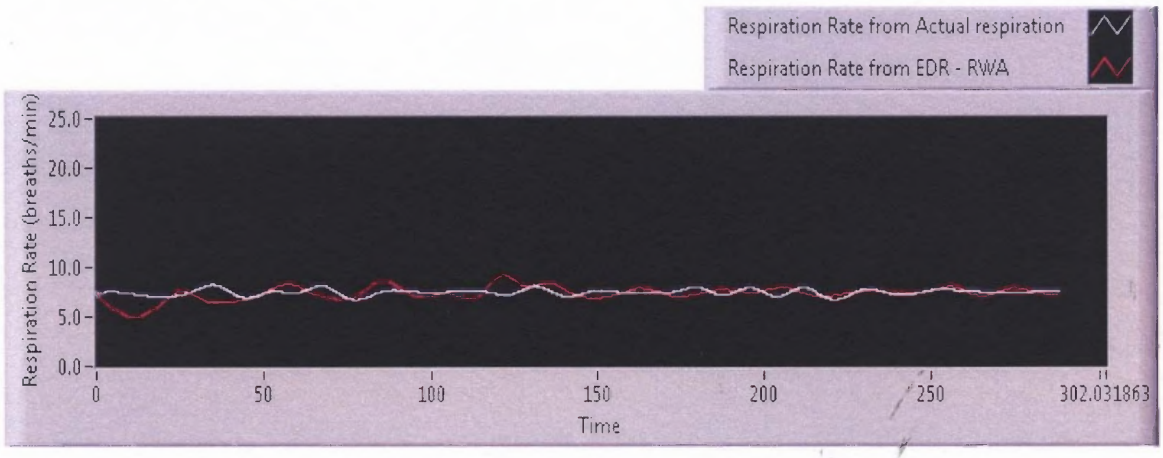

Figure 4.4 Respiration rate signal extracted from actual and derived respiration.

The Tables 4.5, 4.6 and 4.7 show the root mean square error also called root mean square deviation calculated for each subject at different paced breathed samples with respect to actual respiration rate signal. Root mean square error (RMSE) is a frequently used measure of the differences between actual values expected and the values actually observed from the parameter being estimated [31]. The mean standard error for all the samples is about 0.25 breaths/min, which is less than 5 percent. Thus it can be said that the algorithm produces respiration rate signal at a high level of accuracy.

As an outcome of this research a program has been developed which can be used to obtain a continuous respiration rate signal from a single lead ECG with a high level of accuracy.

Table 4.5 RMSE for 8 Breaths/min Paced Breathed Respiration Rate Samples

Subject	RMSE
1A	0.250
1B	0.177
1C	0.311
2A	0.204
2B	0.114
3A	0.139
3B	0.161
4	0.329
5A	0.182
5B	0.463
6A	0.072
6B	0.201
7	0.094
8A	0.094
8B	0.139
9	0.111
10A	0.119
10B	0.135
10C	0.331
Mean	0.190

Note: All units are in breaths/min

Table 4.6 RMSE for 12 Breaths/min Paced Breathed Respiration Rate Samples

Subject	RMSE
1	0.243
2A	0.284
2B	0.621
3A	0.367
3B	0.186
3C	0.234
4A	0.187
4B	0.145
5A	0.309
5B	0.795
5C	0.481
5A	0.254
5B	0.247
6A	0.175
6B	0.210
7	0.118
8A	0.250
8B	0.140
9A	0.158
9B	0.508
10A	0.125
10B	0.135
10C	0.118
Mean	0.273

Note: All units are in breaths/min

Table 4.7 RMSE for 16 Breaths/min Paced Breathed Respiration Rate Samples

Subject	RMSE
1A	0.598
1B	0.451
2A	0.161
2B	0.186
2C	0.487
3A	0.249
3B	0.228
4	0.250
5A	0.228
5B	0.349
6A	0.158
6B	0.107
7	0.616
8A	0.168
9A	0.299
9B	0.361
9C	0.114
Mean	0.294

Note: All units are in breaths/min

4.3 Implementing the ECG Derived Respiration Rate Program

The research was conducted on ECG obtained simultaneously with paced breathed respiration. To demonstrate the use of program in producing a respiration rate signal, few samples of stress data obtained from Dr. Zaim [25] that included exercise and recovery periods were analyzed. In Figures 4.5 - 4.7, two graphs are plotted. The top graph depicts the Heart Rate (HR) (also know as the inter-beat interval (IBI)) vs. time taken during a stress test. In these graphs three segments can be seen: paced breathing, exercise and recovery. For example, Figure 4.5 shows paced breathing from 0 to 400 seconds, exercise from 400 to 900 seconds, and recovery from 900 to 1150 seconds. The bottom graph is a plot of the respiration rate associated with this stress test, developed using RWA method. In all the cases (Figures 4.5-4.7), the respiration rate tracks HR. That is respiration is constant during the paced breathing segment, increases during the exercise period, and drops during the recovery period.

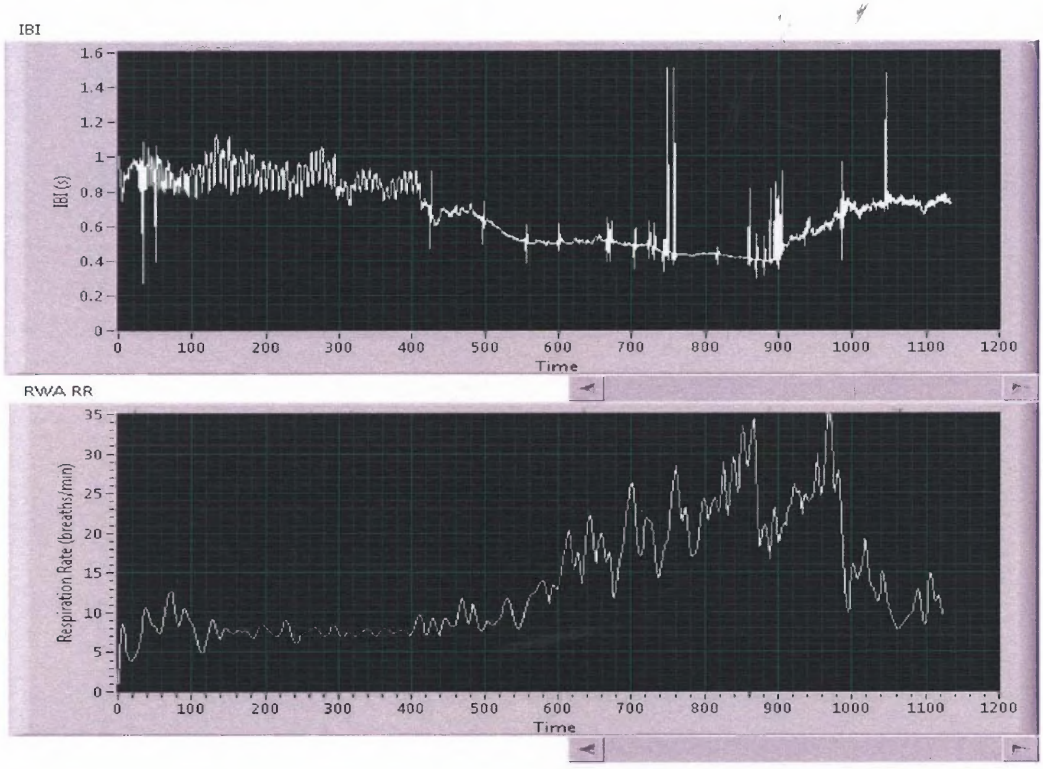

Figure 4.5 IBI and respiration rate plots for stress_sample_1.

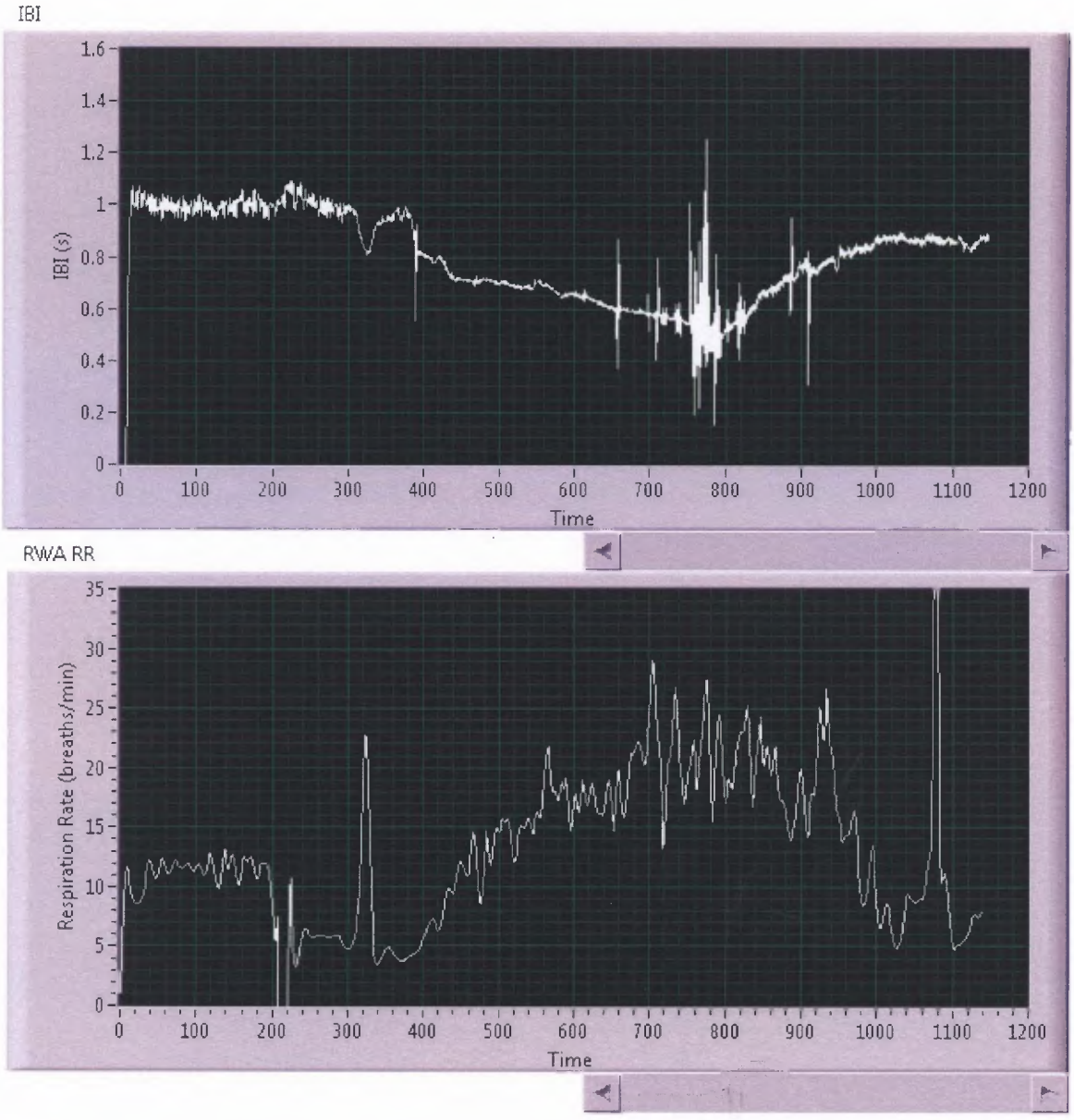

Figure 4.6 IBI and respiration rate plots for stress_sample_2.

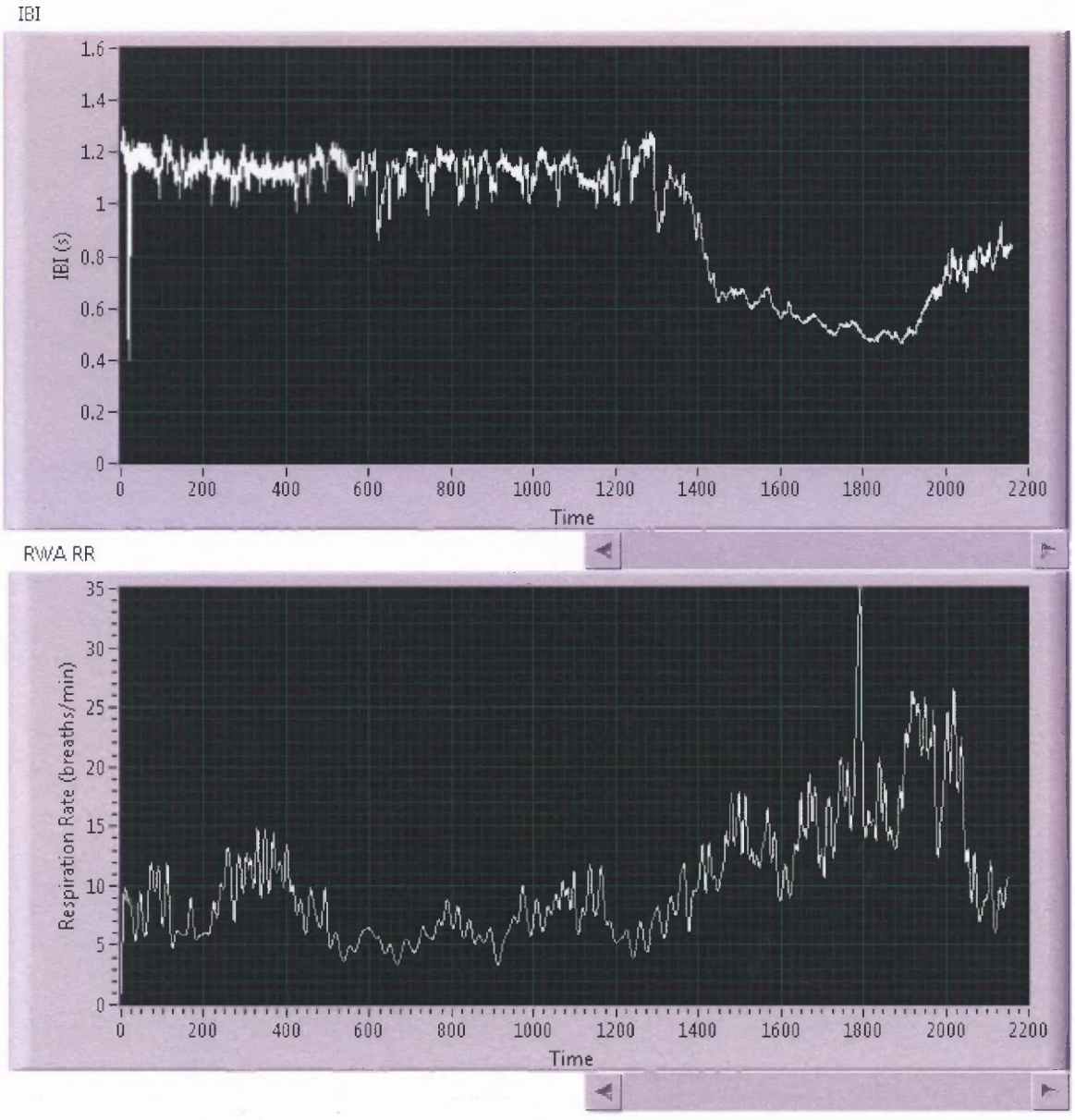

Figure 4.7 IBI and respiration rate plots for stress_sample_3.

CHAPTER 5

CONCLUSION

A preferred technique for deriving respiration signal from a single lead ECG has been identified: the RWA method. The potential advantages of such a technique are its low cost, high convenience, and the ability to simultaneously monitor cardiac and respiratory activity, without the need for cumbersome devices that may interfere with natural breathing during ambulatory monitoring, stress testing, and sleep studies. This technique is also useful to develop a respiration rate signal from a large database of single lead ECGs, where there is no associated respiration signal.

The research shows that R-wave amplitude modulation (RWA) is the best technique for obtaining a single lead EDR signal. R-wave duration (RWD) technique fails under certain situations and is not suitable for single lead EDR. RWA*RWD, the third technique explored, proved to be an inferior technique to RWA, due to the inherent limitations imposed by the RWD technique.

A program written in LabVIEW has been developed to obtain ECG derived respiration rate signal (EDRR) from a single lead ECG.

The single lead EDR accurately measures the frequency of respiratory efforts, but it does not follow the changes in tidal volume. A quantitative explanation of the tidal volume represented by the EDR signal does not seem to be achievable as the depth of modulation on ECG varies from patient to patient [32].

Though most of the work in EDR has been implemented on multi-lead ECG based on electric axis measurement, it has also been suggested that assessing the mean

electrical axis is not as robust a technique as direct assessment of the respiratory modulation [32]. The current research has shown that even a single-lead EDR technique is sufficiently sensitive to identify respiratory events and provide information about respiratory rate. It has also been proven by other researchers that single lead techniques are not unduly affected by postural position [1]. Therefore, the single lead technique developed as a result of this research could be used in applications even where there are significant changes in body positions as in stress test analysis for HRV studies or sleep analysis for apnea studies.

CHAPTER 6

FUTURE WORK

A significant amount of data on exercise and heart rate recovery exists at NJIT which includes single lead ECG but not the associated respiration signal. It is well established that respiratory activity interacts, at the central nervous system level, with the efferent autonomic tone which directly affects heart rate variability by modulating sympathetic and parasympathetic nerve traffic [33]. In addition, the abnormalities in respiratory modulation are an indication of autonomic dysfunction [34]. With the ability to develop a respiratory signal from this database of exercise and heart rate recovery ECGs, a study could be performed to identify the types of respiratory abnormalities that correlate to different kinds of autonomic dysfunction.

HRV analysis is carried out in the frequency domain, using spectral analysis of inter beat intervals (IBI) of ECG and in the time domain, by extracting statistical indexes not related to specific cycle lengths. Parasympathetic activity is primarily reflected in the high-frequency (HF) band of the power spectrum (0.15–0.40Hz) and it is related to the respiratory frequency. The low-frequency (LF) component (0.04–0.15 Hz) is considered by some investigators as a marker of sympathetic modulation [35] and by others as influenced by both the sympathetic and parasympathetic activity [36]. The LF and HF are of particular importance in the clinical environment because the ratio LF/HF is a widely used index of sympathovagal balance [37]. The possibility of selectively and efficiently eliminating the respiratory component from heart rate variability analysis makes it possible to more accurately evaluate the HF role in autonomic nervous system studies.

This is especially important in studying data on heart rate recovery. A technique by Anne Marie Petrock [24] has been developed to remove respiratory component from ECG. However, this technique could not be applied to the extensive dataset that NJIT has from previous exercise studies, since there is no associated respiration signal. This is especially important for future studies on the autonomic changes that occur during heart rate recovery. The methods described in this thesis will enable a respiration signal to be developed from the single lead ECG signals, and thus provide future researchers with the ability to study a respiration-free HF signal during heart rate recovery.

Central and mixed apnea, hypopnea, and tachypnea were identified with confidence using multi-lead ECG, but not all obstructive apneas could be identified. In a subsequent work by Mazzanti and others [2], they provided a quantitative evaluation of the performance of their EDR algorithm in determining obstructive apneas, and concluded that the EDR alone can be useful in determining the presence of obstructive apneas. A drawback of their technique is the need for multiple leads, and also the need for a short training period for the algorithm. The single lead EDR technique could be explored to diagnose sleep apneas where multi-lead techniques have been validated.

Analysis of samples of stress data reveals variability in respiration rate during the stress and recovery periods for a subject. This offers a potential for a study in respiration rate variability during stress test analysis and the underlying physiology behind it. In Figure 6.1, two graphs are presented. The top one depicts the Heart Rate (IBI) vs. time taken during a stress test. In this graph, three segments can be seen: paced breathing from 0 to 400 seconds, exercise from 400 to 900 seconds, and recovery from 900 to 1150

seconds. Below this graph is a graph of the respiration rate associated with this stress test. In this second graph, an example of respiration rate variability is shown.

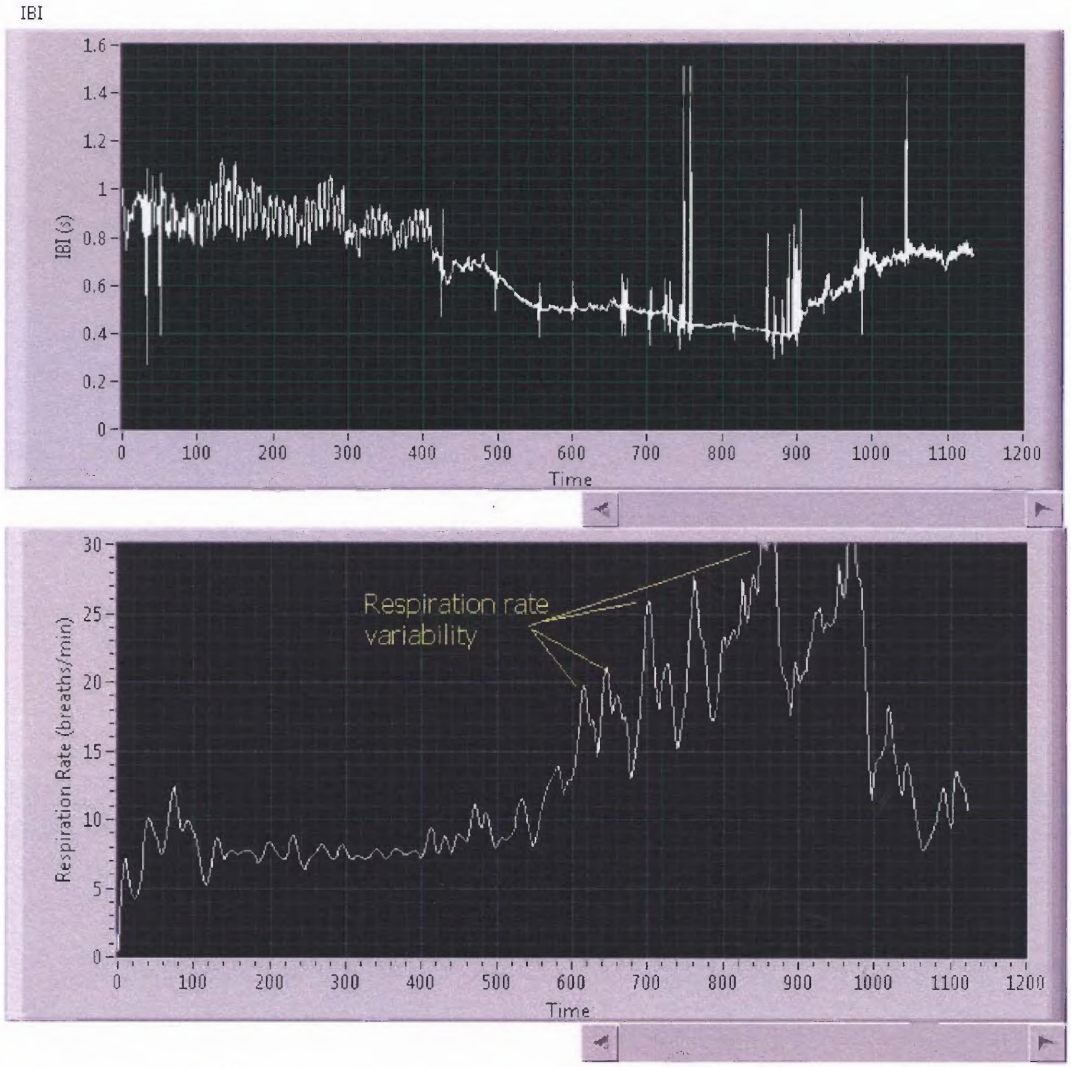

Figure 6.1 Stress test analysis of ECG and respiration (a) IBI (b) Respiration rate.

The single lead EDR accurately measures the frequency of respiratory efforts, but it does not follow the changes in tidal volume [1]. Studies could be performed to accurately measure changes in tidal volume from an EDR.

APPENDIX A

ECG DERIVED RESPIRATION ALGORITHM CODES

The following figures are the LabVIEW codes for algorithms for R wave detection and different EDR methods explored in the research. Every code has a front panel and associated block diagram.

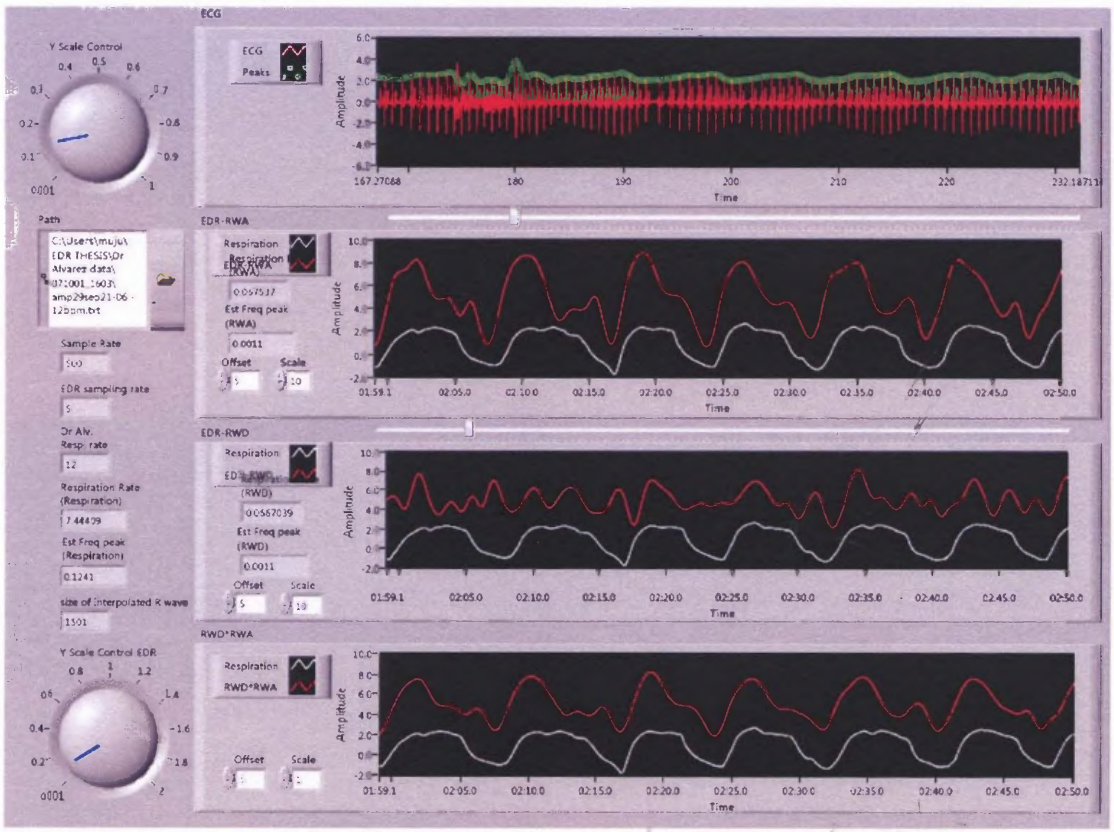

Figure A.1 Front panel of EDR program.

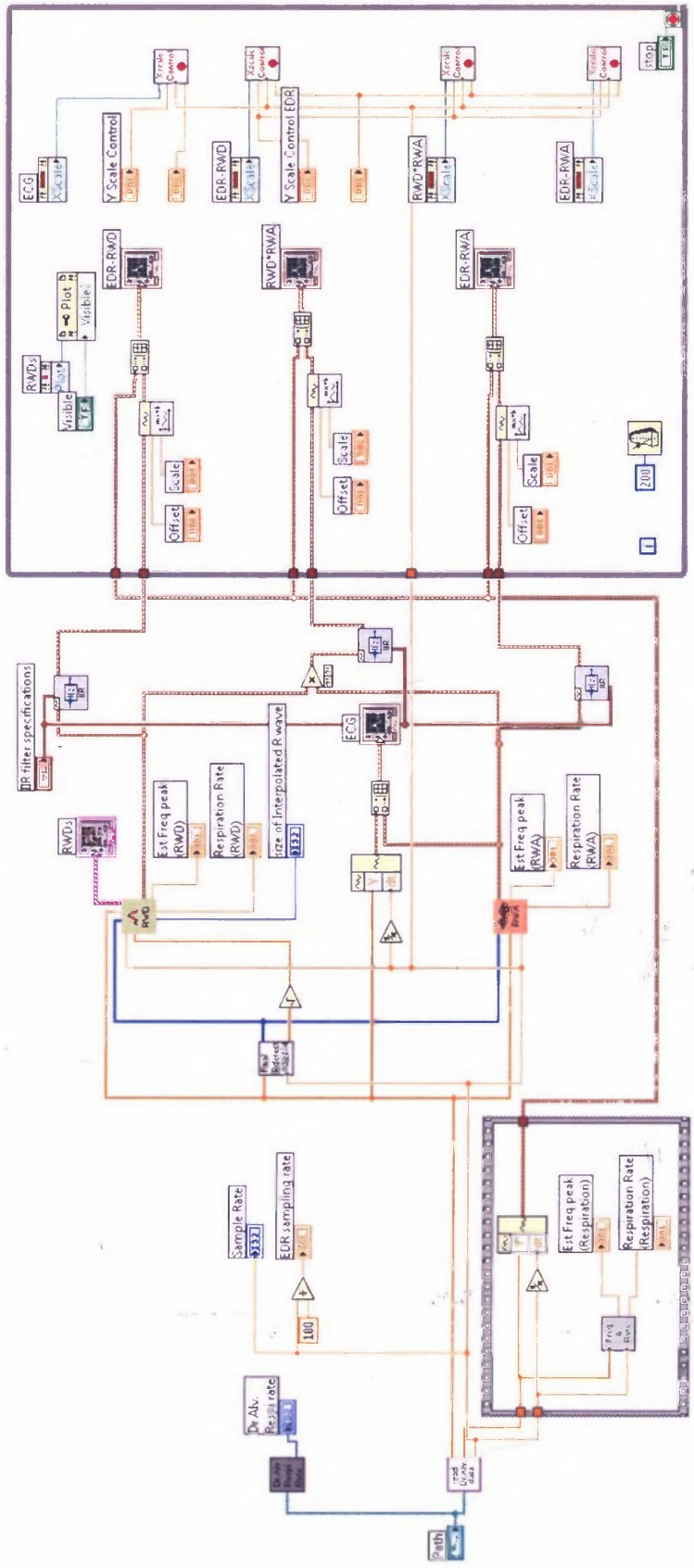

Figure A.2 LabVIEW Block diagram of EDR algorithm.

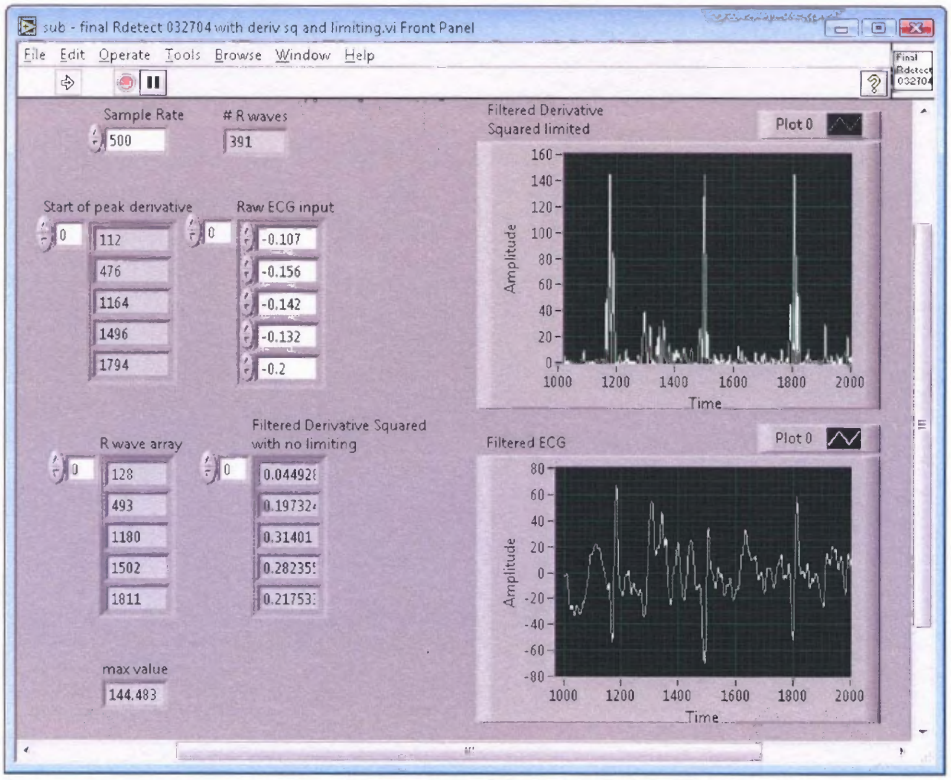

Figure A.3 Front panel of R wave detection algorithm.

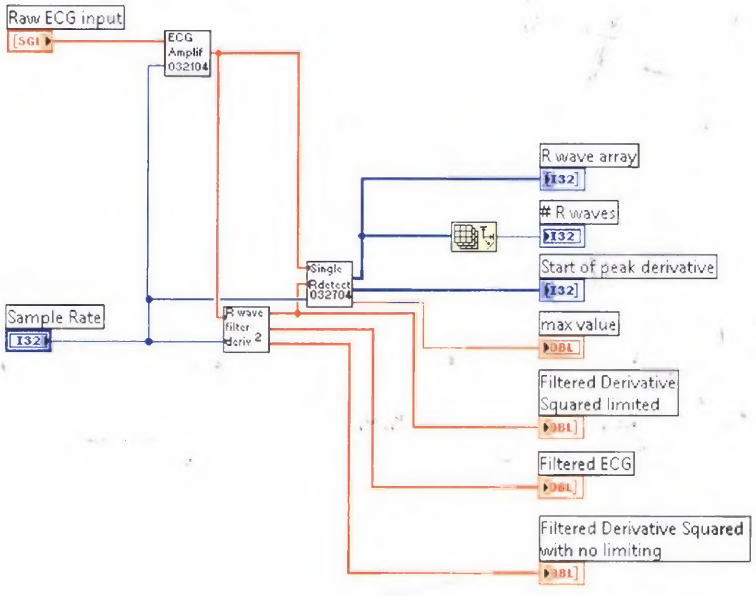

Figure A.4 LabVIEW block diagram of R wave detection algorithm.

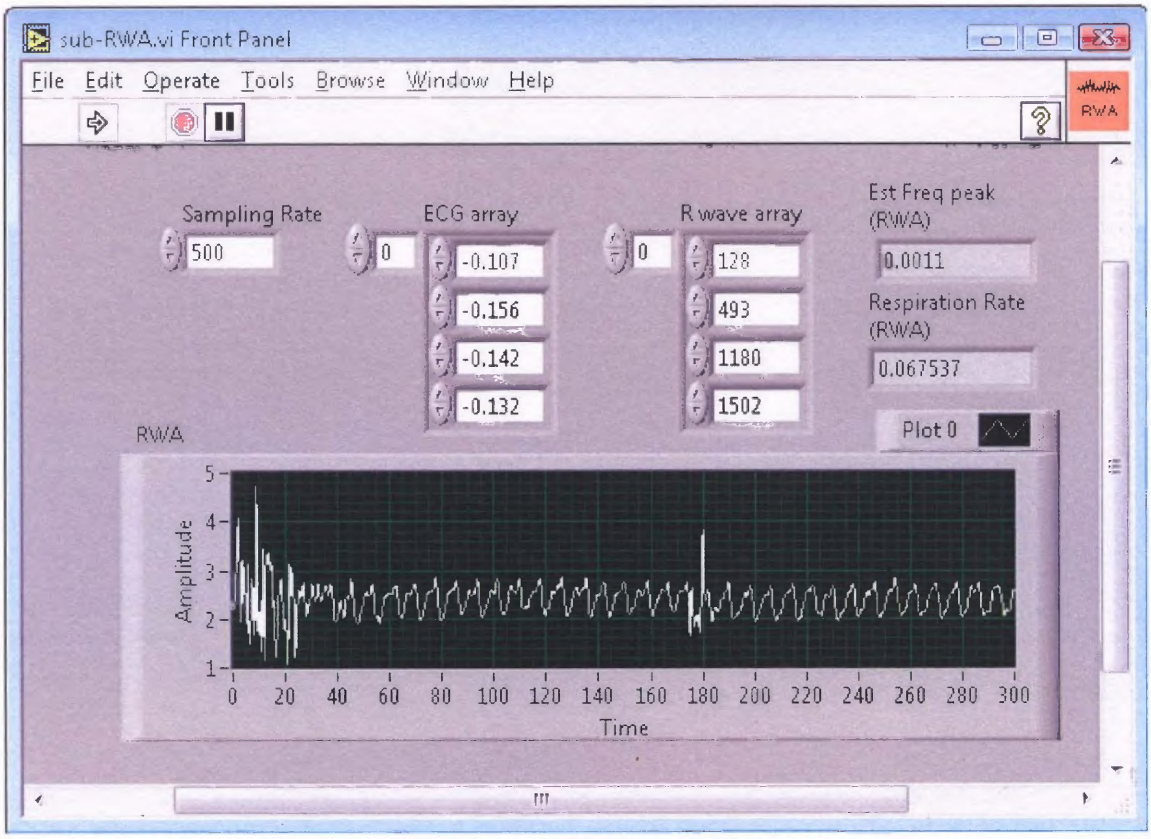

Figure A.5 Front panel of RWA algorithm.

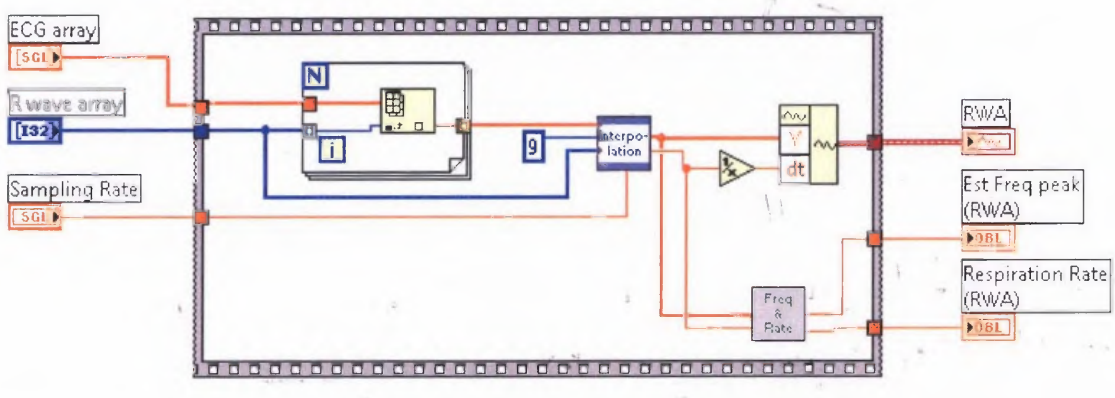

Figure A.6 LabVIEW block diagram of RWA algorithm.

Figure A.7 Front panel of RWD algorithm.

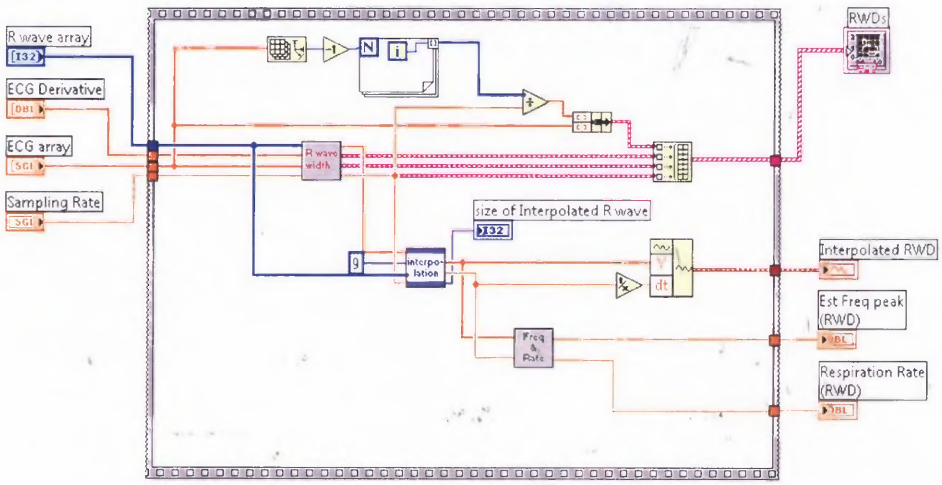

Figure A.8 LabVIEW block diagram of RWD algorithm.

APPENDIX B

RESPIRATION RATE EXTRACTOR ALGORITHM CODES

The following figures are the codes for respiration rate extractor algorithms. FigureB.1 is the front panel of the program developed to derived respiration rate signal from a single lead ECG.

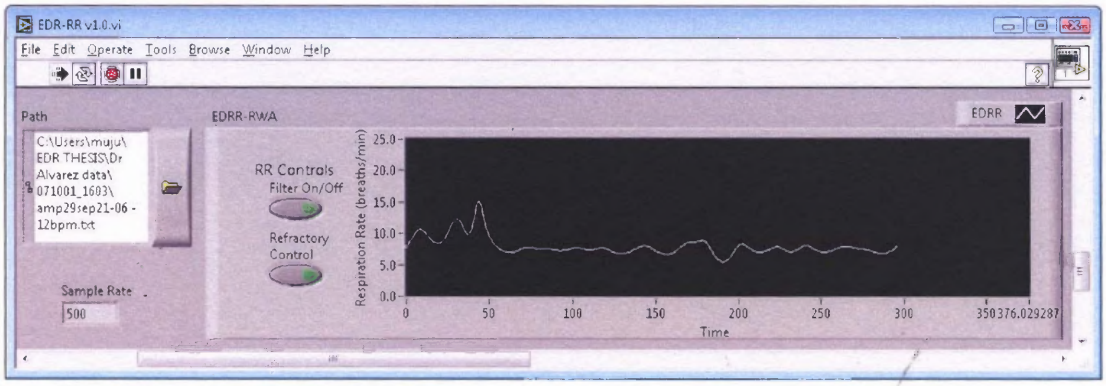

Figure B.1 Front panel of respiration rate extractor algorithm.

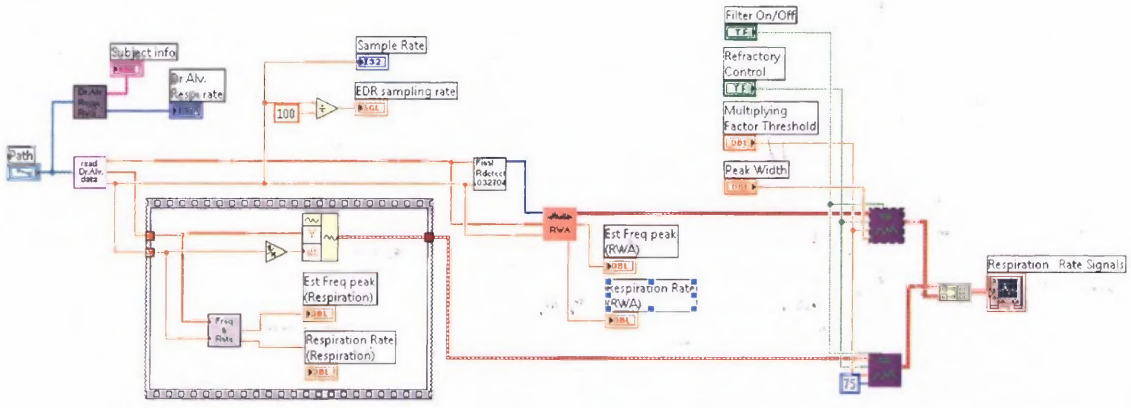

Figure B.2 LabVIEW block diagram of respiration rate detector algorithm.

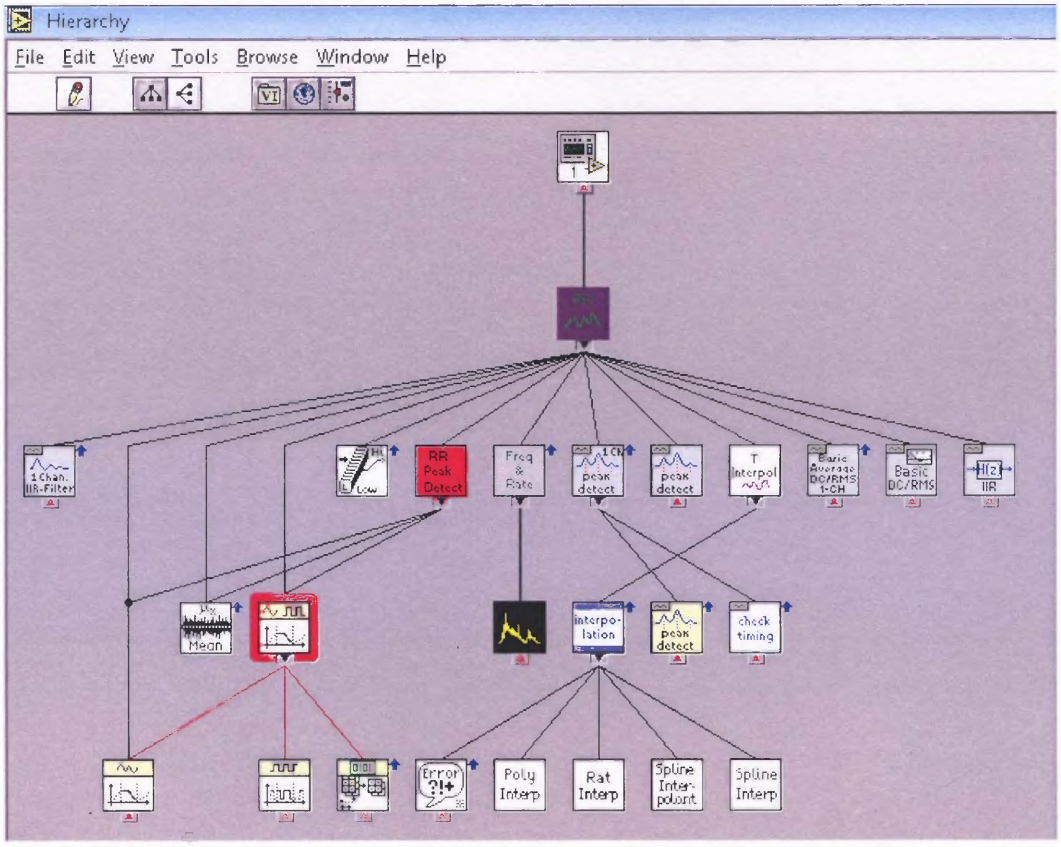

Figure B.3 VI Hierarchy of respiration rate extractor algorithm.

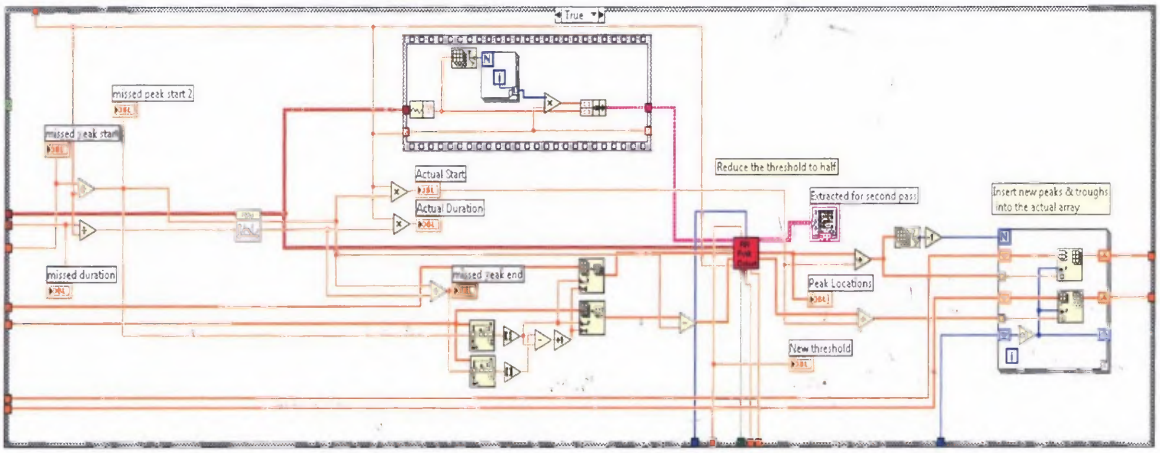

Figure B.4 LabVIEW block diagram of missing peak detector algorithm.

APPENDIX C

IBI AND RESPIRATION VS. TIME PLOTS FOR STRESS SAMPLES

To demonstrate the use of EDRR program, few stress test samples were analyzed and are discussed in Section 4.3. Here are a few more samples. The top graph depicts the Heart Rate (HR) (also know as the inter-beat interval (IBI)) vs. time taken during a stress test. The bottom graph is a plot of the respiration rate vs. time associated for this stress test.

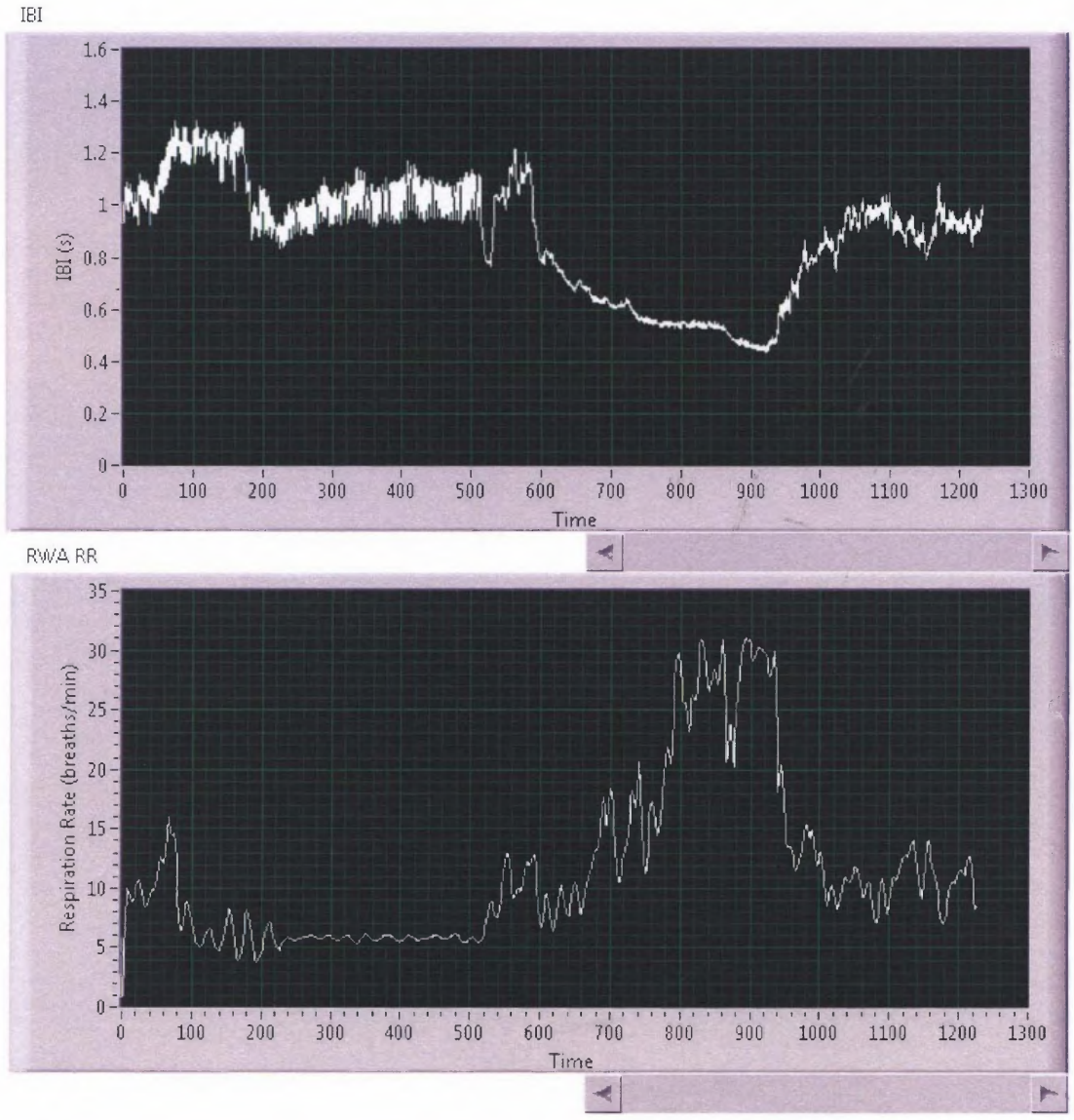

Figure C.1 IBI and respiration rate plots for stress_sample_4.

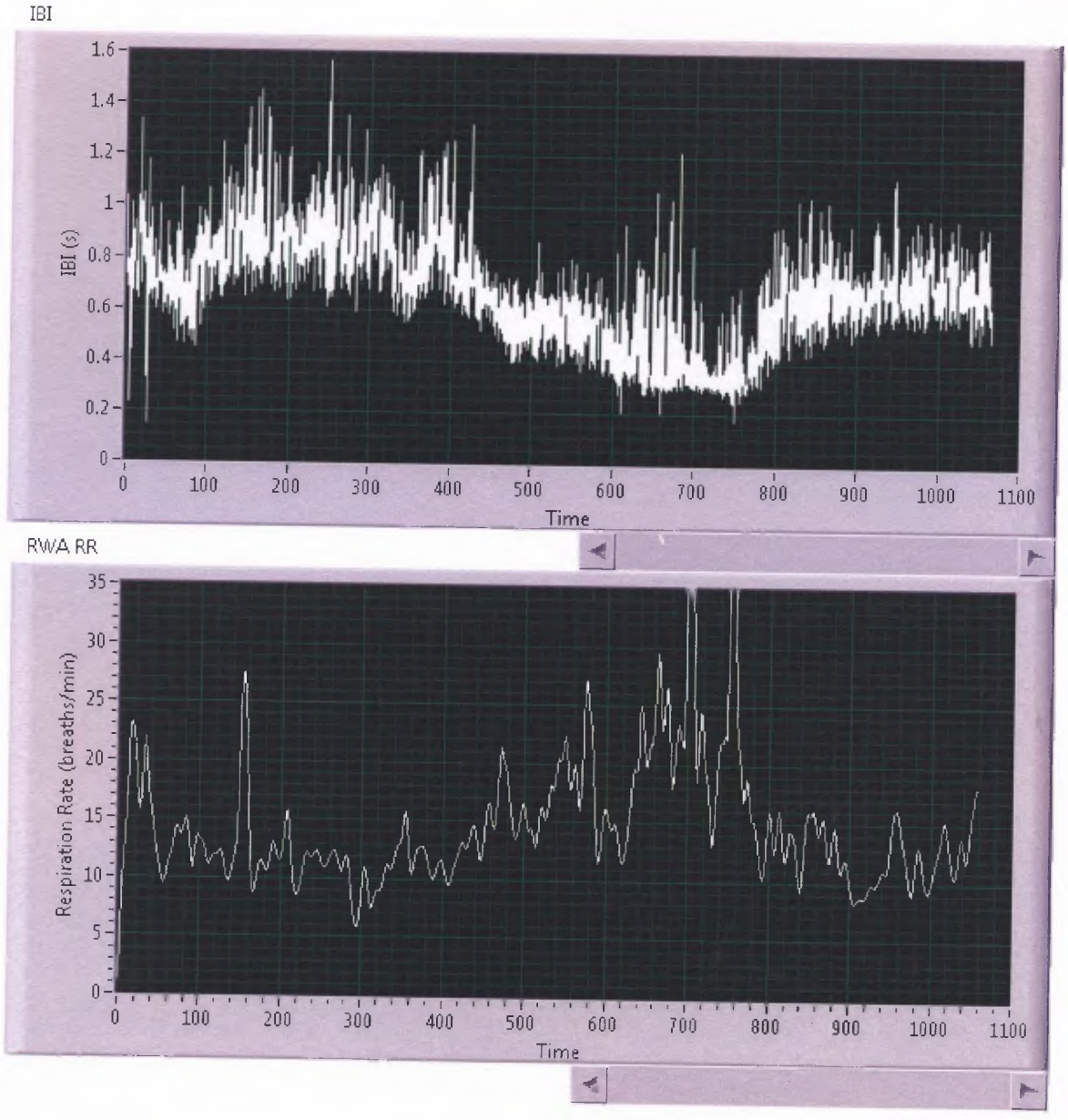

Figure C.2 IBI and respiration rate plots for stress_sample_5.

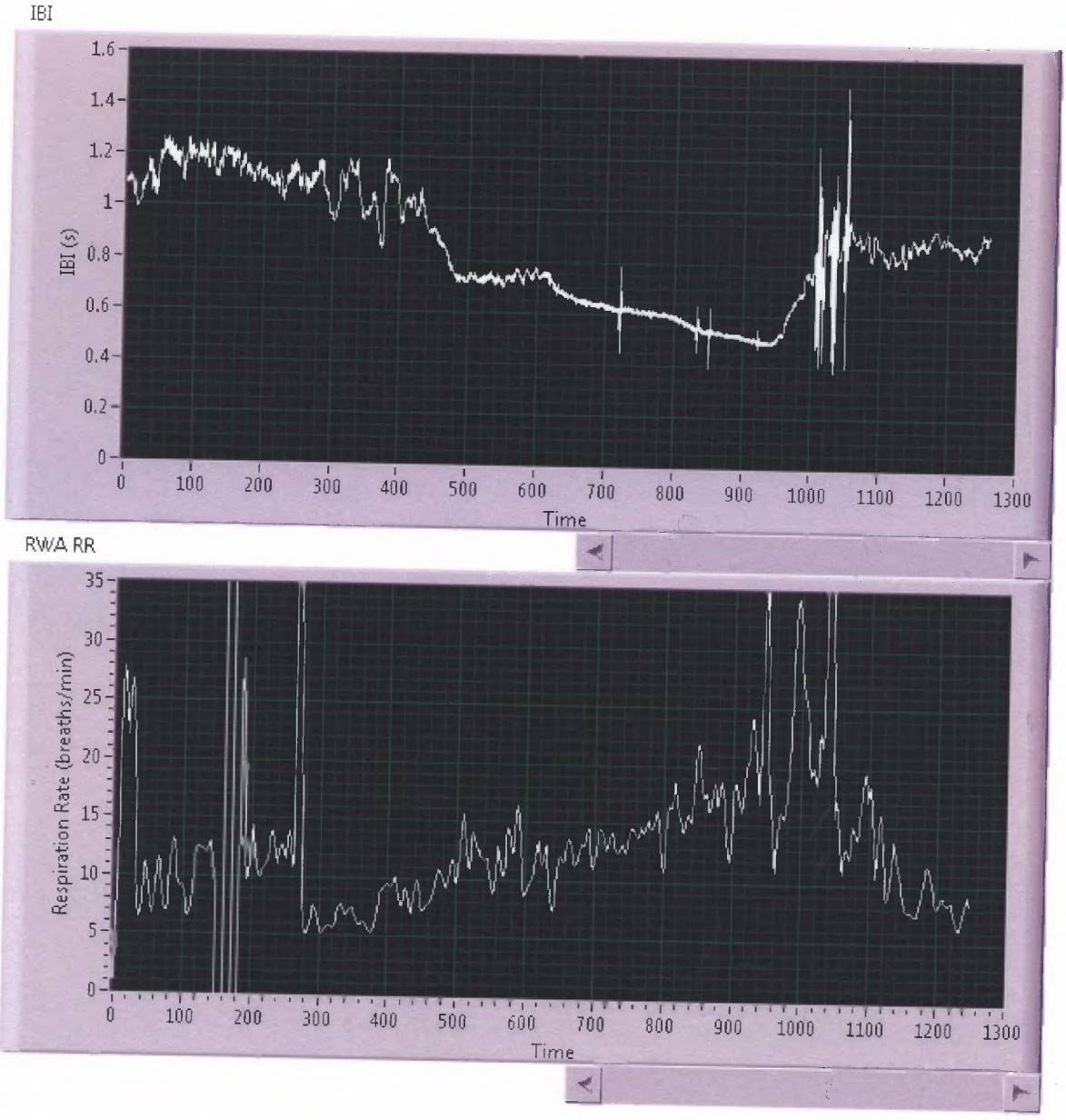

Figure C.3 IBI and respiration rate plots for stress_sample_6.

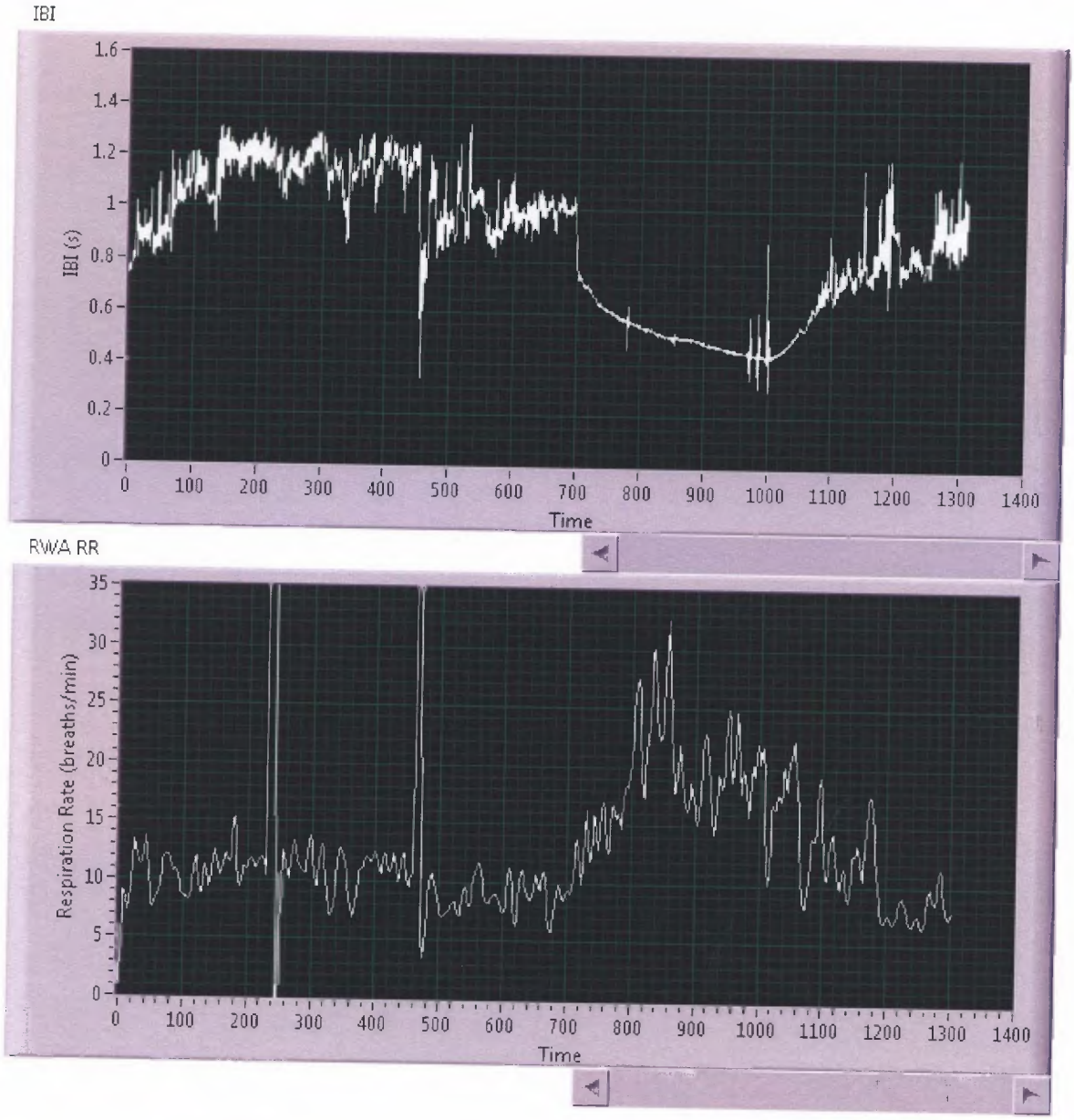

Figure C.4 IBI and respiration rate plots for stress_sample_7.

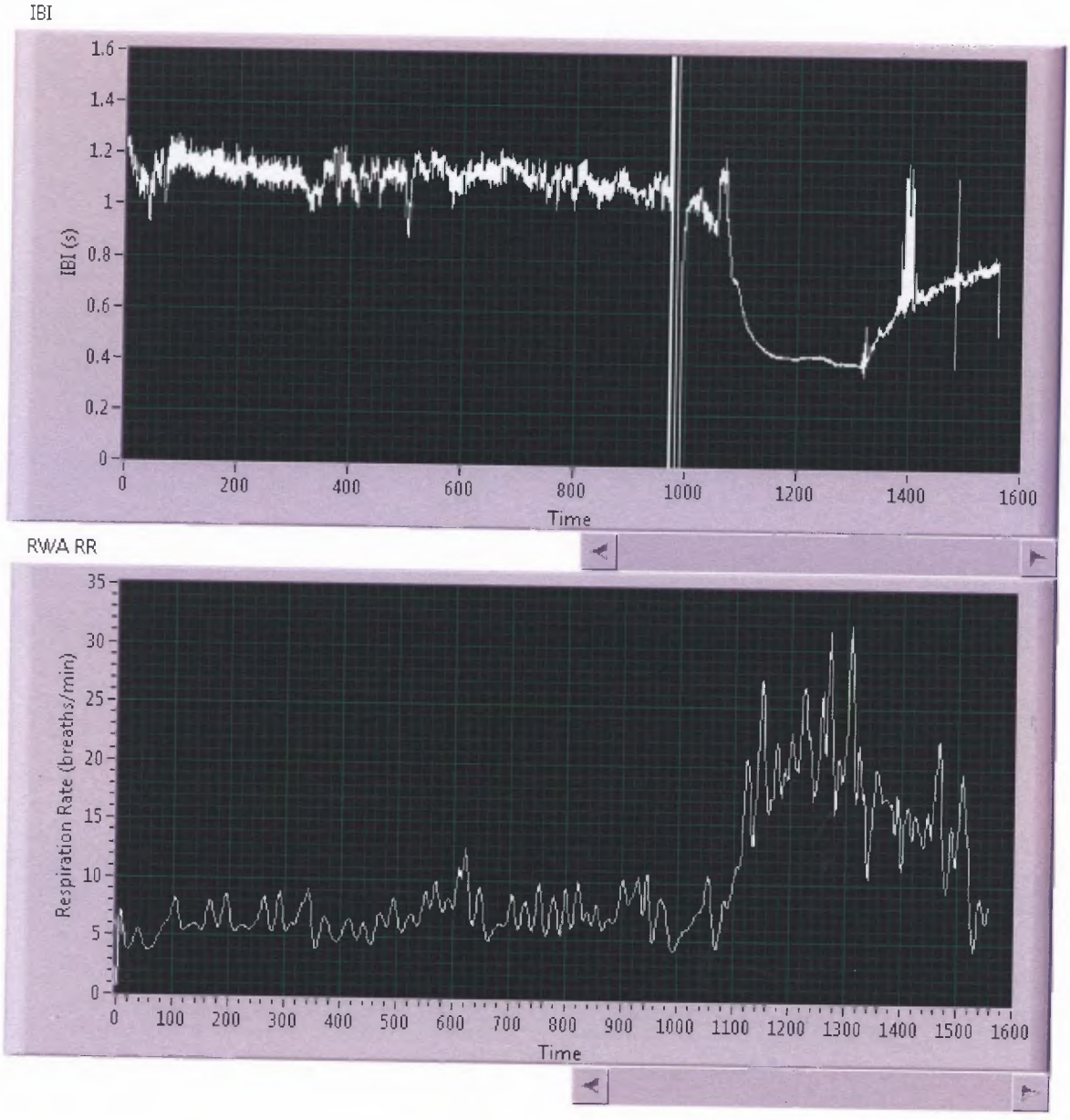

Figure C.5 IBI and respiration rate plots for stress_sample_8.

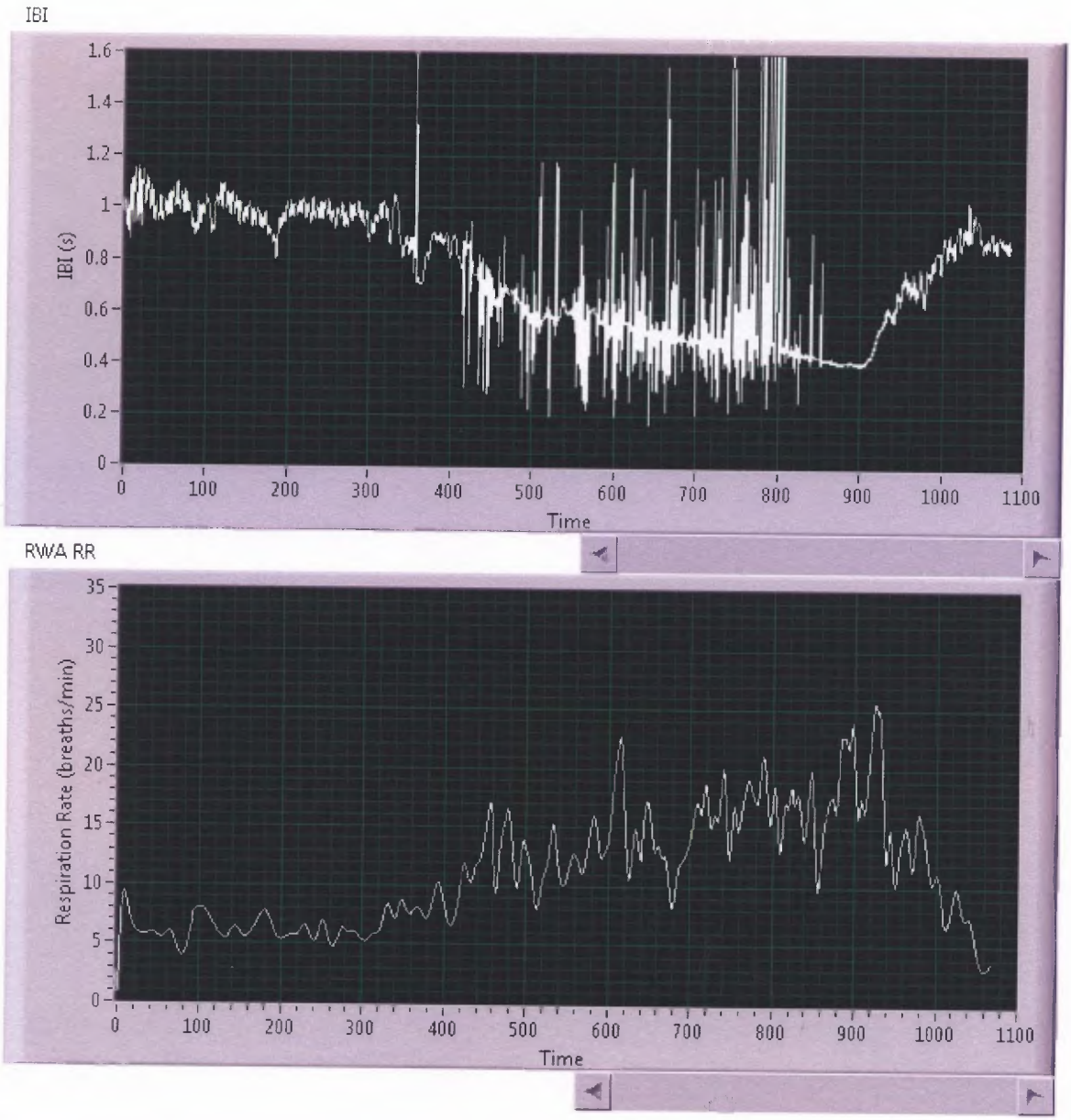

Figure C.6 IBI and respiration rate plots for stress_sample_9.

REFERENCES

[1] G. B. Moody, R. Mark, A. Zoccola, and S. Mantero, "Derivation of respiratory signals from multi-lead ECGs," *Computers in Cardiology,* vol. 12, no. 1, pp. 13-16, 1985.

[2] Association for the Advancement of Medical Instrumentation, "Apnea monitoring by means of thoracic impedance pneumography," Technical Informational Report 4, 1989.

[3] B. Mazzanti, C. Lambertil, and J. de Bie, "Validation of an ECG-derived respiration monitoring method," *Computers in Cardiology*, pp. 613- 616, 21-24 Sept. 2003.

[4] K. Behbehani, S. Vijendra, J. R. Burke, and E. A. Lucas, "An investigation of the mean electrical axis angle and respiration during sleep," in *Proceedings of the Second Joint EMBS/BMES Conference*, vol. 2, October 2002, pp. 1550-1551.

[5] P. de Chazal, C. Heneghan, E. Sheridan, R. Reilly, P. Nolan, and M. O'Malley, "Automated processing of the single lead electrocardiogram for the detection of obstructive sleep apnoea," *IEEE Trans. Biomed. Eng.*, vol. 50, no. 6, pp. 686–696, 2003.

[6] E. de Geus, G. Willemsen, C. Klaver, and L. van Doornen, "Ambulatory measurement of respiratory sinus arrhythmia and respiration rate," *Biological Psychology*, vol. 41, no. 3, pp. 205-227, 1995.

[7] M. Varman, "Computer based biomedical equipment design: an EKG recorder, monitor and simulator," in *Proceedings. 11th IEEE Symposium on Computer-Based Medical Systems*, vol. 12, no. 14, June 1998, pp. 222-227.

[8] S. L. Lipsius, J. Hüser, and L. A. Blatter, "Intracellular Ca2+ release sparks atrial pacemaker activity," *News in Physiological Sciences*, vol. 16, no. 3, pp. 101-106, June 2001.

[9] G. E. Morgan, M. S. Mikhail, and M. J. Murray, *Clinical Anesthesiology*, Medical, 2005.

[10] R. S. Khandpur, *Handbook of Biomedical Instrumentation*, New Delhi: Tata McGraw-Hill, 2003.

[11] Website: http://www.healthsystem.virginia.edu/Internet/afibcenter/images/normal_ heart.jpg, April 2008.

[12] Website: http://upload.wikimedia.org/wikipedia/commons/thumb/9/9e/SinusRhythm Labels.svg/300px-SinusRhythmLabels.svg.png, April 2008.

[13] R. E. Klabunde, *Cardiovascular Physiology Concepts*, Lippincott Williams and Wilkins, 2005.

[14] Website: http://anginapectorisonline.com/cssimg/12_lead_ecg_placement.jpg, April 2008.

[15] A. Guyton, and J. Hall, *Textbook of Medical Physiology*, Philadelphia: W. B. Saunders and Company, 1996.

[16] Website: http://www.britannica.com/eb/art-99770, April 2008.

[17] Website: http://www.mis.atr.jp/past/sem/img_shared/sensors.jpg, April 2008.

[18] R. S. Khandpur, *Biomedical Instrumentation: Technology and Applications*, New Delhi: Tata McGraw-Hill, 2006.

[19] Website: http://www.rochestermed.com/Ulfw1x1.jpg, April 2008.

[20] L. Zhao, S. Reisman, and T. Findley, "Derivation of respiration from electrocardiogram during heart rate variability studies," *Computers in Cardiology*, pp. 53-56, Sept. 1994.

[21] G. Furman, Z. Shinar, A. Baharav, and S. Akselrod, "Electrocardiogram derived respiration during sleep," *Computers in Cardiology*, pp. 351-354, Sept. 25-28, 2005.

[22] Z. Shinar, A. Baharav, and S. Akselrod, "R wave duration as a measure of body position changes during sleep," *Computers in Cardiology,* pp. 49-52, 1999.

[23] S. Gupta, J. John, *Virtual Instrumentation Using LabVIEW*, McGraw Hill, 2005.

[24] A. M. Petrock, "Central and peripheral autonomic influences: Analysis of cardio-pulmonary dynamics using novel wavelet statistical methods," Ph. D. Dissertation, New Jersey Institute of Technology, Newark, NJ, USA, May 2007.

[25] Dr. S. Zaim, University of Medicine and Dentistry, NJ, Medical School, Newark, NJ, 2008.

[26] P. Asselin, "Relationship between the autonomic nervous system and the recovering heart post exercise using heart rate variability," M.S. thesis, New Jersey Institute of Technology, Newark, NJ, USA, May 2005.

[27] A. Wilson, C. Franks, and I. Freeston, "Algorithms for the detection of breaths from respiratory waveform recordings of infants," *Medical and Biological Engineering and Computing*, vol. 20, no. 3, May 1982.

[28] R. B. D'Agostino, L. M. Sullivan, and A. S. Beiser, "*Introductory Applied Biostatistics*," Thomson, Brooks/Cole, 2005.

[29] J. P. Clayton, *The Concept of Correlation: Paul Tillich and the Possibility of a Mediating Theology*, Walter de Gruyter, 1980.

[30] J. M. Bland and D. G. Altman, "Statistical methods for assessing agreement between two methods of clinical measurement," *Lancet*, i, pp. 307-310, 1986.

[31] Clementz , W . Iacono , and W . Grove, "The construct validity of root-mean-square error for quantifying smooth-pursuit eye tracking abnormalities in schizophrenia," *Biological Psychiatry*, vol. 39, no. 6, pp. 448-450, March 1996.

[32] C. O'Brien and C. Heneghan, "A comparison of algorithms for estimation of a respiratory signal from the surface electrocardiogram," *Computers in Biology and Medicine,* vol. 37, pp. 305-314, 2007.

[33] J. B. West, *Physiological Basis of Medical Practice*, Baltimore: Williams and Wilkins, 1937.

[34] L. Bernardi. C. Porta, A Gabutti, L. Spicuzza, and P. Sleight, "Modulatory effects of respiration," *Autonomic Neuroscience*, vol. 90, no. 1, pp. 47-56, 20 July 2001.

[35] P. Sleight and P. Bernardi, "Sympathovagal balance," Circulation, vol. 98, no. 23, pp. 2640-2640, 1998.

[36] D. L. Eckberg, "Sympathovagal balance: a critical appraisal," *Circulation*, vol. 96, pp. 3224-32, 1997.

[37] R. Balocchi, D. Menicucci, E. Santarcangelo, L. Sebastiani, A. Gemignani, B. Ghelarducci, and M. Varanini, "Deriving the respiratory sinus arrhythmia from the heartbeat time series using empirical mode decomposition," *Solitons and Fractals,* vol. 20, pp. 171-177, 2004.